

Outlier detection and a tail-adjusted boxplot based on extreme value theory

Shrijita Bhattacharya *and Jan Beirlant†

December 6, 2019

Abstract

Whether an extreme observation is an outlier or not, depends strongly on the corresponding tail behaviour of the underlying distribution. We develop an automatic, data-driven method to identify extreme tail behaviour that deviates from the intermediate and central characteristics. This allows for detecting extreme outliers or sets of extreme data that show less spread than the bulk of the data. To this end we extend a testing method proposed in *Bhattacharya et al. (2019)* for the specific case of heavy tailed models, to all max-domains of attraction. Consequently we propose a tail-adjusted boxplot which yields a more accurate representation of possible outliers. Several examples and simulation results illustrate the finite sample behaviour of this approach.

1 Introduction

The identification of outliers has become an important topic in several statistical methods and fields of application, such as the general field of novelty detection, next to for instance climatology and cyber crime. It then is important to judge if an observation or a set of observations can be explained from the model fitted to the bulk of the data or from a deviating model.

The classical boxplot introduced by *Tukey (1977)* is the prime classical tool indicating *potential* outliers, marking individual data with an asterisk or dot when it has a distance larger than 1.5 interquartile range (*IQR*) from the corresponding quartile Q_1 or Q_3 . In fact, when the underlying distribution of the data is normal, $X \sim \mathcal{N}(\mu, \sigma^2)$, the probability for an extreme normal observation to be wrongly indicated as an outlier in a classical boxplot is very small: at the right hand side tail of the distribution for large enough sample sizes it is approximately given by

$$\mathbb{P}(X > Q_3 + 1.5IQR) = \mathbb{P}(X > [\mu + 0.67\sigma] + 1.5[1.34\sigma]) = \mathbb{P}(Z > 2.68) = 0.0037.$$

*Department of Statistics and Probability, Michigan State University, C419 Wells Hall, 619 Red Cedar Rd East Lansing, MI 48824, bhatta61@msu.edu

†Department of Mathematics, KULeuven, Department of Mathematical Statistics and Actuarial Science, University of the Free State

However, for distributions with a tail heavier than the normal model the probability for a data point to be indicated by a dot is growing. The probability $\mathbb{P}(X > Q_R + 1.5IQR)$ equals 0.05 for an exponential distribution, while for a lognormal distribution, i.e. $\log X \sim \mathcal{N}(\mu, \sigma^2)$, this probability raises up to 0.08 when $\sigma = 1$ and 0.16 when $\sigma = 2$. For the Pareto distribution with distribution function $F(x) = 1 - x^{-\alpha}$ ($x > 1, \alpha > 0$), this probability amounts to 0.073 with $\alpha = 4$ and 0.16 when $\alpha = 1$. In such cases the boxplot grossly overestimates the number of *real* outliers.

At the other side of the spectrum, considering tails with a finite right endpoint, the probability of indicating an observation as a potential outlier is typically lower, for instance 0 for the uniform distribution on $(0,1)$, since then real outliers can well be situated below $Q_3 + 1.5IQR$.

From this we can conclude that the classical boxplot can be a misleading tool for outlier detection, while it is often erroneously used for that purpose. In *Hubert and Vandervieren (2008)* the classical boxplot was adjusted for skewness using some robust skewness estimators. However, in general, tail heaviness cannot be determined on the basis of a skewness measure. Here extreme value methodology is used to detect outliers making direct use of tail heaviness indicators.

Extreme value theory (EVT) is a natural methodology to describe and estimate tail heaviness. EVT starts from considering the limit distribution of the maximum of sequences of independent and identically observations X_1, X_2, \dots, X_n :

$$\mathbb{P}(a_n^{-1}(\max_{i=1, \dots, n} X_i - b_n) \leq y) \rightarrow G_\xi(y) = \exp(-(1 + \xi y)^{-1/\xi}), \quad 1 + \xi y > 0, \quad \text{as } n \rightarrow \infty, \quad (1.1)$$

for some sequences $(a_n > 0)$ and (b_n) , where the generalized extreme value distributions (GEV) with distribution function (df) G_ξ are the only possible limit distributions. The GEV family is parametrized by the extreme value index (EVI) $\xi \in \mathbb{R}$. In case $\xi = 0$ the limit GEV is given by $G_0(y) = \exp(-\exp(-y))$, $y \in \mathbb{R}$. The EVI is a measure of the tail-heaviness of the distribution of X with a larger value of ξ implying a heavier tail described by the right tail function (RTF) $\bar{F}(x) = 1 - F(x) = \mathbb{P}(X > x)$.

In the specific case $\xi > 0$ the distributions F satisfying the limit result (1.1), composing the Fréchet domain of attraction, are given by the set of Pareto-type distributions with RTF given by

$$\bar{F}(x) = \mathbb{P}(X > x) = x^{-\frac{1}{\xi}} \ell(x), \quad (1.2)$$

where ℓ is a slowly varying function at infinity, i.e.

$$\frac{\ell(ty)}{\ell(t)} \rightarrow 1 \text{ as } t \rightarrow \infty, \text{ for every } y > 1. \quad (1.3)$$

The estimation of ξ under (1.2) has received most attention starting with the Hill (1975) estimator

$$H_k = \frac{1}{k} \sum_{j=1}^k \log X_{n-j+1,n} - \log X_{n-k,n} = \frac{1}{k} \sum_{j=1}^k V_j, \quad (1.4)$$

where $X_{1,n} \leq X_{2,n} \leq \dots \leq X_{n,n}$ denote the ordered observations and V_j denote the weighted log-spacings

$$V_j = j \log \frac{X_{n-j+1,n}}{X_{n-j,n}}, \quad j = 1, \dots, n-1. \quad (1.5)$$

The set of distributions F for which (1.1) holds with $\xi = 0$, the Gumbel domain, mainly contains exponentially decreasing tails such as normal, gamma, Weibull and lognormal models. The Weibull domain corresponding to $\xi < 0$ consists of distributions with a finite endpoint. Estimation of the EVI with $\xi \in \mathbb{R}$ has also been studied in detail, and here we can refer to *Beirlant et al.* (2004) and *de Haan and Ferreira* (2006) for general reviews. In this paper we make use of the generalized Hill estimator of $\xi \in \mathbb{R}$ given by

$$GH_k = \frac{1}{k} \sum_{j=1}^k \log(X_{n-j+1,n} H_j) - \log(X_{n-k,n} H_{k+1}). \quad (1.6)$$

This estimator can be visualized through linear regression on the extreme right k points of the **generalized QQ-plot** defined as

$$\left(\log \left(\frac{j+1}{n+1} \right), \log(X_{n-j+1,n} H_j) \right), \quad j = 1, \dots, n-1.$$

Indeed this plot can be shown to be ultimately linear and the slope can be measured with GH_k (see section 5.2.3 in *Beirlant et al.* (2004)).

While the EVT methods as described above concentrate on the right hand side tail, the method can be extended to the left hand side tail by applying it for instance to the transformed variable $1/X$ in case of positive data, or to $-X$ in case of negative values to the left of the median.

In this paper we generalize the approach from *Bhattacharya et al.* (2019) and show that the trimmed Hill statistic

$$\begin{aligned} H_{k_0,k} &= \frac{k_0}{k-k_0} \log \left(\frac{X_{n-k_0,n}}{X_{n-k,n}} \right) + \frac{1}{k-k_0} \sum_{i=k_0+1}^k \log \left(\frac{X_{n-i+1,n}}{X_{n-k,n}} \right) \\ &= \frac{1}{k-k_0} \sum_{j=k_0+1}^k V_j, \quad 0 \leq k_0 < k \leq n, \end{aligned} \quad (1.7)$$

and the corresponding test for outliers based on the ratio

$$T_{k_0,k} = \frac{(k-k_0-1)H_{k_0+1,k}}{(k-k_0)H_{k_0,k}}, \quad 0 \leq k_0 < k, \quad (1.8)$$

can still be used to develop an outlier detection method in the general case $\xi \in \mathbb{R}$, while *Bhattacharya et al.* (2019) considered $\xi > 0$. An estimate of the number of outliers is then obtained by a sequential

method identifying the largest value of k_0 for which $T_{k_0,k}$ yields a significant value. Using this outlier detection mechanism, we can construct a *tail-adjusted boxplot* (see section 2.2 below) where the whiskers extend from the upper quartile Q_3 up to the largest value among all non-outlying observations, and similarly for the left whisker below Q_1 .

Next to obtaining a value of k_0 , an estimate of $\xi \in \mathbb{R}$ is of course very informative as it will offer a first guess concerning the type of the underlying tail. While estimation of the EVI in the presence of outliers is not the main goal of this paper, we will need a trimmed version of the generalized Hill estimator GH_k as a starting value in the outlier detection procedure. Given a value of k_0 , let

$$GH_{k_0,k} = \frac{1}{k - k_0} \sum_{j=k_0+1}^k \log(X_{n-j+1,n}H_{k_0,j}) - \log(X_{n-k,n}H_{k_0,k+1}), \quad 0 \leq k_0 < k \leq n, \quad (1.9)$$

where, for $k_0 < j$,

$$H_{k_0,j} = \frac{1}{j - k_0} \sum_{i=k_0+1}^j \log X_{n-i+1,n} - \log X_{n-j,n}, \quad (1.10)$$

which is a Hill-type estimator based on the observations $X_{n-j,n} \leq X_{n-j+1,n} \leq \dots \leq X_{n-k_0,n}$. Plotting the estimates $GH_{k_0,k}$ as a function of k_0 will be used as a visual device in identifying change points (such as outliers or shifts of regime) in the data characteristics. The plot of $GH_{k_0,k}$ as a function of k_0 for some particular values of k will be referred to as the **diagnostic k_0 plot**.

In order to illustrate the importance of tail behaviour in the determination of outliers, we consider precipitation data from France as considered in *Bernard et al.* (2013). Weekly maxima of hourly precipitation at 92 French stations during the fall season from 1993 to 2011 are considered, as provided by the French meteorological service Météo-France. The stations were chosen in function of their quality and to have a fairly homogeneous coverage of France. Here we consider the data from Chamonix and Uzein, respectively situated in that South-East and South-West of France. *Bernard et al.* (2013) situated the Chamonix case in the Gumbel domain while the Uzein data appeared to be Pareto distributed. In order to avoid issues with ties a small uniform noise $U(-0.01, 0.01)$ was added to the data. The diagnostic k_0 plots for both stations will be given in section 4.

Concerning the Chamonix precipitation data (N 45.93°, E 6.88°) *Bernard et al.* (2013) proposed the estimate 0.01 for ξ , so that this right hand tail is situated near the Gumbel domain. The linear fit on the exponential QQ-plot of the Chamonix data given in Figure 1 indeed shows that the tail behavior is close to exponential. While the classical boxplot indicates 4 potential outliers, the method presented here indicates two deviating points which arises from the fact that the second and third largest points are almost equal. When enlarging the random noise the top two values are no longer flagged as outliers.

In contrast to the Chamonix data, the precipitation at Uzein (N 43.38° E -0.42°) appears to have a Pareto-type behaviour as concluded already in *Bernard et al.* (2013) with an EVI estimate of 0.35.

This is also confirmed by a linear regression fit on the top 64 points of the Pareto QQ-plot in Figure 2. Here the classical boxplot indicates 8 possible outliers. The present tail-adjusted approach indicates 13 possible outliers when using the full Pareto-type character in the top 64 data points. While the top 13 observations can be stated to be in line with the Pareto fit as indicated in the Pareto QQ-plot in Figure 2, these data are indeed separated from the bulk of the data as can be observed from the time plot in Figure 2 .

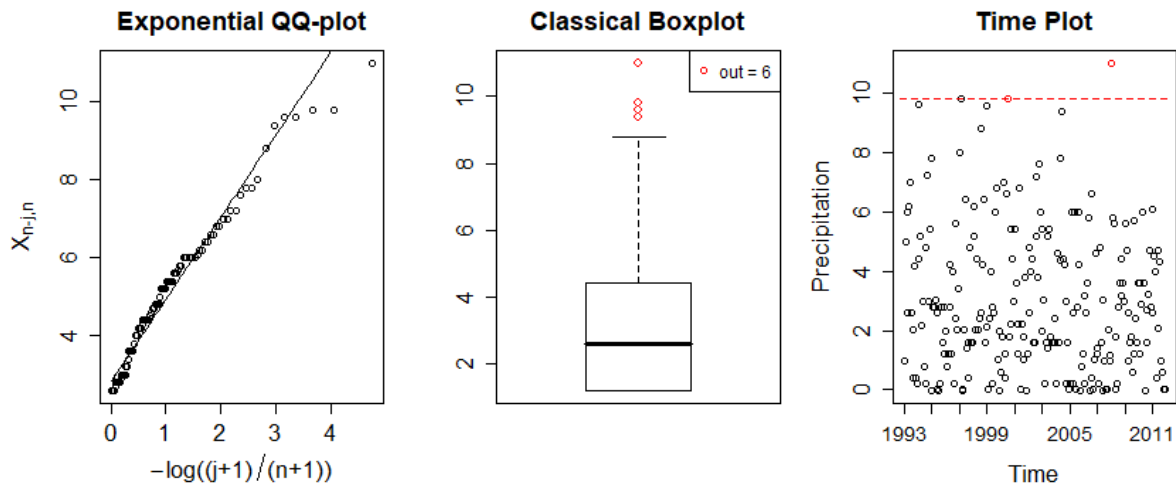


Figure 1: *Precipitation* data from Chamonix station. *Left:* Exponential QQ-plot. *Middle:* Classical boxplot. *Right:* Time plot with indication of the outlier threshold for the tail-adjusted method when using the top 114 data.

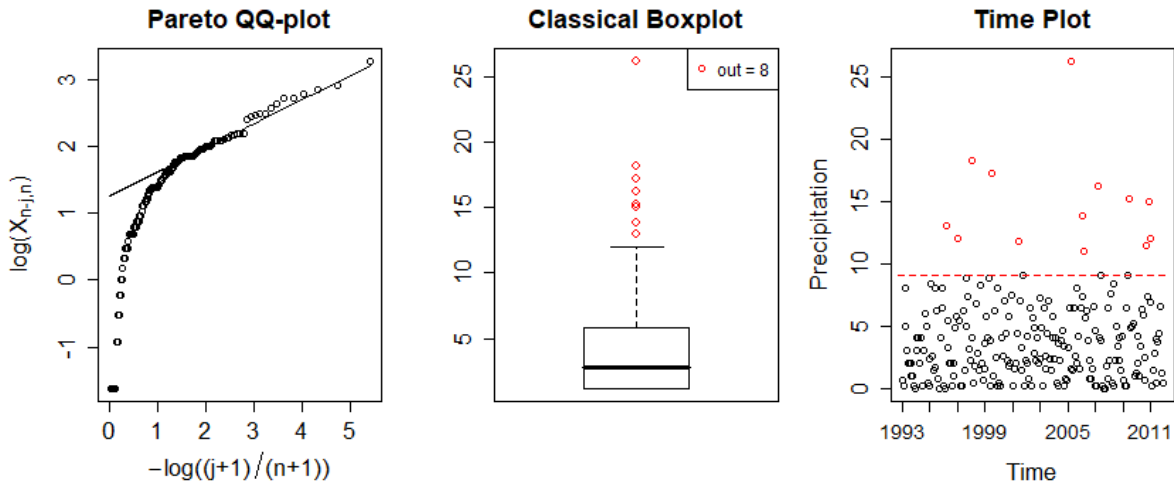


Figure 2: *Precipitation* data from Uzein station. *Left*: Pareto QQ-plot. *Middle*: Classical boxplot. *Right*: Time plot with indication of the outlier threshold for the tail-adjusted method when using the top 64 data.

The rest of the paper is organized as follows. In section 2 we develop tests for outliers based on extreme value methodology whatever the tail behaviour of the underlying distribution is. We provide mathematical justification for the proposed procedure, the proof of which are deferred to the Appendix. In section 3 we report on a simulation study, while in section 4 we discuss several case studies in order to illustrate the practical use of the proposed methods. Proofs are deferred to the Appendix, as well as some parts of the simulation study.

2 Testing for outliers under extreme value conditions

The main goal of this paper is to generalize the approach from *Bhattacharya et al. (2019)* based on $T_{k_0,k}$ from $\xi > 0$ to $\xi \in \mathbb{R}$. To this end we derive distributional properties of the trimmed Hill statistic $H_{k_0,k}$ and the test statistic $T_{k_0,k}$ for all three domains of attraction. This then leads to an algorithm for automated selection of the number of outliers k_0 .

2.1 On the distribution of $H_{k_0,k}$ and $T_{k_0,k}$

We here consider asymptotic properties as $k, n \rightarrow \infty$ with $k/n \rightarrow 0$ and $k_0/k \rightarrow 0$. We use conditions under which (1.1) holds in terms of the tail quantile function $U(x) = F^{\leftarrow}(1 - x^{-1})$ where F^{\leftarrow} denotes the quantile function which is defined as the left continuous inverse of the df F . Given that the Hill statistic is defined in terms of the logarithm of the empirical quantiles, we use the equivalent condition of (1.1) in terms of $\log U$, as can be found for instance in section 3.5 in *de Haan and Ferreira (2006)*:

for some positive function q

$$\frac{\log U(tx) - \log U(t)}{q(t)} \rightarrow \Psi_{\gamma_-}(x) := \frac{x^{\xi_-} - 1}{\xi_-} \text{ as } t \rightarrow \infty, \text{ for every } x > 1,$$

where $\xi_- = \min(\xi, 0)$ and where $\Psi_{\gamma_-}(x)$ reads as $\log x$ in case $\xi \geq 0$ or $\xi_- = 0$.

In order to study the bias of the trimmed Hill $H_{k_0, k}$ and $T_{k_0, k}$ statistic we will in fact need a second order condition as can be found in Chapter 3 of *de Haan and Ferreira (2006)*: as $t \rightarrow \infty$

$$\frac{\frac{\log U(tx) - \log U(t)}{q(t)} - \frac{x^{\xi_-} - 1}{\xi_-}}{Q(t)} \rightarrow \int_1^x s^{\xi_- - 1} \int_1^s u^{\rho - 1} du ds, \text{ for all } x > 0, \quad (2.1)$$

with Q not changing sign eventually and $Q(t) \rightarrow 0$ as $t \rightarrow \infty$, and $\rho \leq 0$.

By Theorem 2.3.6 in *de Haan and Ferreira (2006)*, functions $q_0(t)$ and $Q_0(t)$ can be constructed following (3.5.12) and (3.5.13) in that reference, so that for every $\epsilon, \delta > 0$, there exists $t_0 = t_0(\epsilon, \delta)$ such that for all $t, t \geq t_0$ and $x > 1$:

$$\left| \frac{\frac{\log U(tx) - \log U(t)}{q_0(t)} - \Psi_{\xi_-}(x)}{Q_0(t)} - \Phi_{\xi_-, \rho}(x) \right| \leq \epsilon x^{\xi_- + \rho + \delta}, \quad (2.2)$$

with $\Phi_{\xi_-, \rho}(x)$ defined as

$$\Phi_{\xi_-, \rho}(x) = \begin{cases} \frac{x^{\xi_- + \rho} - 1}{\xi_- + \rho}, & \xi_- + \rho < 0, \rho < 0, \\ \frac{x^{\xi_-}}{\xi_-} \log x, & \xi_- < 0, \rho = 0, \\ \frac{1}{2} (\log x)^2, & \xi_- = 0, \rho = 0. \end{cases}$$

To obtain an approximation of the distribution of the test statistic $T_{k_0, k}$, we first state a general representation theorem for the trimmed Hill statistics $H_{k_0, k}$ after which we can provide an asymptotic representation of $T_{k_0, k}$.

Theorem 2.1. *Suppose (2.1) holds for some $\xi \in \mathbb{R}$, $\rho \leq 0$. Then for $k/n \rightarrow 0$, $k_0 = o(k)$, and*

$$\sqrt{k}Q(n/k) \rightarrow \lambda \quad (2.3)$$

with λ finite, we have

- when $\xi \geq 0$,

$$\frac{k - k_0}{k} \frac{H_{k_0, k}}{q_0(Y_{n-k, n})} \stackrel{d}{=} \frac{1}{k} \sum_{i=k_0+1}^k Z_i + \frac{\lambda c_{0, \rho}}{\sqrt{k}} + o_{\mathbb{P}}(k^{-1/2})$$

- when $\xi < 0$,

$$\frac{k - k_0}{k} \frac{H_{k_0, k}}{q_0(Y_{n-k, n})} \stackrel{d}{=} \frac{k_0}{k\xi} (\exp(\xi \sum_{j=k_0+1}^k Z_j/j) - 1) + \frac{1}{k\xi} \sum_{i=k_0}^{k-1} (\exp(\xi \sum_{j=i+1}^k Z_j/j) - 1) + \frac{\lambda c_{\xi, \rho}}{\sqrt{k}} + o_{\mathbb{P}}(k^{-1/2})$$

where the constants $c_{0, \rho}$ and $c_{\xi, \rho}$ satisfy

$$c_{0, \rho} = \begin{cases} \frac{1}{\rho(1-\rho)} \left(1 - \left(\frac{k_0}{k}\right)^{1-\rho}\right), & \rho < 0 \\ \left(1 - \frac{k_0}{k} \left(1 + \log \frac{k_0}{k}\right)\right), & \rho = 0 \end{cases}; \quad c_{\xi, \rho} = \begin{cases} \frac{1}{\rho(1-\xi-\rho)} \left(1 - \left(\frac{k_0}{k}\right)^{1-\xi-\rho}\right), & \rho < 0, \\ \frac{1}{\xi(1-\xi)^2} \left(1 - \left(\frac{k_0}{k}\right)^{1-\xi} \left(1 + \xi(1-\xi) \log \frac{k_0}{k}\right)\right), & \rho = 0. \end{cases} \quad (2.4)$$

Next, we consider the asymptotic distribution of $T_{k_0, k}$.

Theorem 2.2. *Suppose (2.1) holds for some $\xi \in \mathbb{R}$, $\rho \leq 0$. Then for $k/n \rightarrow 0$, $k_0 = o(k)$, and*

$$\sqrt{k}Q(n/k) \rightarrow \lambda$$

with λ finite, we have for any $\delta > 0$ that

- when $\xi \geq 0$

$$1 - T_{k_0, k} \stackrel{d}{=} \frac{Z_{k_0+1} \left(1 + O_{\mathbb{P}}(k^{-1/2}) + O_{\mathbb{P}}(k^{\rho+\delta-1/2} k_0^{1-\rho-\delta})\right)}{\sum_{j=k_0+1}^k Z_j}$$

- when $\xi < 0$

$$1 - T_{k_0, k} \stackrel{d}{=} \left(\frac{k_0 + 1}{k}\right) \xi \frac{(k_0 + 1) (\exp(\frac{\xi Z_{k_0+1}}{k_0+1}) - 1) \left(1 + O_{\mathbb{P}}(k^{-1/2}) + O_{\mathbb{P}}(k^{\rho+\delta-1/2} k_0^{1-\rho-\delta})\right)}{k_0 (\exp(\sum_{j=k_0+1}^k \frac{\xi Z_j}{j}) - 1) + \sum_{i=k_0}^{k-1} (\exp(\sum_{j=i+1}^k \frac{\xi Z_j}{j}) - 1)}$$

where Z_1, Z_2, \dots are independent standard exponentially distributed.

Remark 2.1. Note that in case $\xi \geq 0$ the statistic $1 - T_{k_0, k}$ is approximated by a Beta($k - k_0 - 1, 1$) distribution. This corresponds with Proposition 4.1 in *Bhattacharya et al. (2019)* which was obtained for $\xi > 0$ with ℓ in (1.2) constant.

The next result follows from Theorem 2.2 using the central limit theorem on $k^{-1} \sum_{j=k_0+1}^k Z_j$ and $k^{-1} (k_0 \exp(\sum_{j=k_0+1}^k \xi Z_j/j) + \sum_{i=k_0}^{k-1} \exp(\sum_{j=i+1}^k \xi Z_j/j) - k)$.

Corollary 2.3. *Under the conditions of Theorem 2.3, for any $\delta > 0$ we have*

$$\left(\frac{k}{k_0 + 1}\right)^{1-\xi_-} (1 - T_{k_0, k}) \stackrel{d}{=} (1 - \xi_-) h_{\xi_-} \left(\frac{Z}{k_0 + 1}\right) \left(1 + O_{\mathbb{P}}(k^{-1/2}) + O_{\mathbb{P}}(k^{\rho+\delta-1/2} k_0^{1-\rho-\delta})\right),$$

with Z standard exponentially distributed and $h_{\xi_-}(u) = (e^{u\xi_-} - 1)/\xi_-$ if $\xi_- < 0$, and $h_{\xi_-}(u) = u$ otherwise.

Corollary 2.4. *Under the conditions of Theorem 2.3, for any $\delta > 0$ we have that*

1. for $\xi \geq 0$ and $k_0 = o(k^{(1/2-\rho-\delta)/(1-\rho-\delta)})$,

$$k(1 - T_{k_0,k}) \xrightarrow{d} Z,$$

2. for $\xi < 0$, $k_0 = o(k^{(1/2-\rho-\delta)/(1-\rho-\delta)})$ and $k_0 \rightarrow \infty$,

$$k \left(\frac{k_0 + 1}{k} \right)^\xi (1 - T_{k_0,k}) \xrightarrow{d} (1 - \xi)Z,$$

3. for $\xi < 0$ and $k_0 \rightarrow M < \infty$,

$$\left(\frac{k}{k_0 + 1} \right)^{1-\xi} (1 - T_{k_0,k}) \xrightarrow{d} \frac{1-\xi}{\xi} \left(e^{\frac{\xi Z}{M}} - 1 \right),$$

with Z standard exponentially distributed.

2.2 Algorithm for automated selection

Here we describe the formal methodology for estimating the number of outliers. In view of Corollary 2.3, note that the distribution of $T_{k_0,k}$ depends on the true value of ξ . Setting

$$E_{k_0,k}^\xi := \begin{cases} k(1 - T_{k_0,k}), & \xi > 0 \\ \frac{k_0+1}{\xi} \log \left(1 + \left(\frac{k}{k_0+1} \right)^{1-\xi} \frac{\xi}{1-\xi} (1 - T_{k_0,k}) \right), & \xi \leq 0, \end{cases}$$

with $k_0 = 0, 1, \dots, k-2$, we obtain from Corollary 2.3 that $E_{k_0,k}^\xi$ is approximately standard exponentially distributed for large enough values of k and n with k/n and k_0/k sufficiently small, which implies that

$$U_{k_0,k}^\xi = 2|0.5 - \exp(-E_{k_0,k}^\xi)|, \quad k_0 = 0, 1, \dots, k-2 \quad (2.5)$$

approximately follows the uniform (0,1) distribution. The main items in the selection algorithm are given next.

An initial estimator of ξ . Assuming an upper bound k_0^* for the number of outliers k_0 , one can construct a crude initial estimate of ξ based on $GH_{k_0^*,k^*}$ as defined in (1.9) using some appropriate values k_0^* and k^* where k^* can be different from the value k used in (2.5).

Imputing $GH_{k_0^*,k^*}$ for ξ in (2.5), we can identify k_0 as the largest value j for which $U_{j,k}^\xi$ fails a test for uniformity on significance level α_j for some sequence $(\alpha_j; j = 0, \dots, k-2)$ discussed below. Numerically, one can thus write

$$\widehat{k}_0^{\{0\}} = \operatorname{argmax}_{j=1, \dots, k_0^*} \{j : U_{j,k}^{GH_{k_0^*,k^*}} > 1 - \alpha_j\} \quad (2.6)$$

where the argmax of an empty set is set to 0. With this value $\widehat{k}_0^{\{0\}}$ we define a revised estimate of ξ as

$$\widehat{\xi} = GH_{\widehat{k}_0^{\{0\}}, k^*}. \quad (2.7)$$

Note that the estimator in (2.7) is not an optimal estimator of ξ . This is because GH_{i, k^*} is asymptotically suboptimal especially at large values of i . Thus, one must guard against choosing large values of k_0^* in defining the initial estimate of ξ . On the other hand if k_0^* is less than the true number of outliers, $GH_{k_0^*, k^*}$ will involve outlier observations, thereby resulting in a severely biased estimate of ξ . Extensive analysis showed that $k_0^* = o(k^{*1/2})$ works well in practice. A more specific proposal is discussed in the simulation section.

Estimation of k_0 . Based on the initial estimate $\widehat{\xi}$ from (2.7), we obtain an improved estimate of k_0 :

$$\widehat{k}_0^{\{1\}} = \operatorname{argmax}_{j=1, \dots, k_0^*} \{j : U_{j, k}^{\widehat{\xi}} > 1 - \alpha_j\}. \quad (2.8)$$

Groups of outliers. One can extend the above approach to allow for different groups of outliers. In this direction, we define

$$\mathcal{V} = \{j \in 1, \dots, \widehat{k}_0^{\{1\}} : U_{j, k}^{\widehat{\xi}} > 1 - \alpha_j\}$$

which are the possible points at which a significance is detected among the outliers. Let $0 = v_0 \leq v_1 \leq v_2 \leq \dots \leq v_{|\mathcal{V}|} = \widehat{k}_0^{\{1\}}$ denote the entries of $|\mathcal{V}|$ in increasing order.

With an a priori assumption that there are no more than $V \leq |\mathcal{V}|$ regime outliers, we next define V regime of outliers as

$$\widetilde{\ell}_{\{r\}} = \begin{cases} \{v_{r-1}, \dots, v_r\}, & r = 1, \dots, V-1 \\ \{v_{r-1}, \dots, v_{|\mathcal{V}|}\}, & r = V \end{cases} \quad (2.9)$$

with $\widetilde{\ell}_{\{r\}} = \phi$.

This then leads to the following detection algorithm and consequently a tail-adjusted boxplot.

Algorithm 1 Domain Adapted Sequential Testing (DAST)

- 1: Input k, k^*, k_0^* and V .
- 2: Set $\tilde{V} = 0$ and $\hat{\ell}^{\{0\}} = 0$.
- 3: Set $\alpha_j \in (0, 1)$, $j = 0, 1, \dots, k-2$ satisfying

$$\prod_{j=0}^{k-2} (1 - \alpha_j) = 1 - q \quad (2.10)$$

- 4: Compute $\hat{k}_0^{\{0\}}$ and $\hat{\xi}$ using Relations (2.6) and (2.7) respectively.
- 5: Compute $U_{j,k}^{\hat{\xi}}$ as in Relation (2.5).
- 6: Compute $\hat{k}_0^{\{1\}}$ as in Relation (2.8).
- 7: If $\tilde{k}_0^{\{1\}} = 0$ goto step 10, else define

$$\mathcal{V} = \{j \in 1, \dots, \hat{k}_0^{\{1\}} \mid U_{j,k}^{\hat{\xi}} > 1 - \alpha_j\}.$$

- 8: Set $\tilde{V} = \min(|\mathcal{V}|, V)$
- 9: If $\tilde{V} = 1$, define $\ell_{\{1\}} = \hat{k}_0^{\{1\}}$ and goto step 10, else define

$$\tilde{\ell}_{\{r\}} = \begin{cases} \{v_{r-1}, \dots, v_r\}, & r = 1, \dots, \tilde{V} - 1 \\ \{v_{r-1}, \dots, v_{|\mathcal{V}|}\}, & r = \tilde{V} \end{cases}$$

where $0 = v_0 \leq v_1 \leq v_2 \leq \dots \leq v_{|\mathcal{V}|} = \hat{k}_0^{\{1\}}$ denote the entries of $|\mathcal{V}|$ in increasing order.

- 10: Return $\{\hat{\ell}_{\{0\}}, \dots, \hat{\ell}_{\{\tilde{V}\}}\}$
-

Choice of α_j . As in *Bhattacharya et al. (2019)*, the levels α_j in the above algorithm are chosen as

$$\alpha_j = 1 - (1 - q)^{ca^{k-j-1}}, \quad j = 0, \dots, k-2, \quad (2.11)$$

with $a > 1$ and $c = 1 / \sum_{j=0}^{k-2} a^{k-j-1}$. This choice of α_j satisfies (2.10), which implies

$$P_{k_0=0}[\hat{k}_0 > 0] = q,$$

so that the algorithm is well calibrated (see Proposition 2.9 in *Bhattacharya et al. (2019)*). In addition, this choice puts less weight on large values of j which implies that large values of j are less likely to be chosen over smaller ones. This guards against encountering spurious values of \hat{k}_0 close to k . Extensive sensitivity analysis with a variety of sequential tests indicate that the choice of levels as in (2.11) with $a = 1.2$ works well in practice.

Tail-adjusted boxplot. We propose to apply the DAST algorithm to obtain the right tail outliers, while the bottom outliers are determined by applying the DAST algorithm to the right tail of the

transformed random variable $1/X$ in case of positive data, and $-X$ in case of negative left tail data. One can indicate the different sets of outliers as detected by the above algorithm using different symbols such as $+$, \circ , \dots . The whiskers of the tail-adjusted boxplot extends from the upper, respectively lower, quartile to the extreme observations just below, respectively above, the set of identified outliers. In the case studies below, we also report the p-values of the different sets of outliers. For each regime $\tilde{\ell}_r$, these p-values are equal to $U_{v_r, k}^{\hat{\xi}}$ with $\hat{\xi}$ and v_r as in (2.7) and (2.9) respectively.

3 Simulations.

In this section, we study the accuracy of the DAST algorithm (see Algorithm 1 of Section 2.2) as an estimator of the true number of outliers k_0 . The parameters a and q are set at 1.2 and 0.05 respectively. We concentrate only on one regime of outliers, i.e. V is set equal to 1 in Algorithm 1.

Measures of Performance: The performance of \hat{k}_0 as generated from the DAST algorithm is evaluated in terms of its expected value, $E(\hat{k}_0)$ and the standard deviation $\sqrt{\text{Var}(\hat{k}_0)}$. These computations are based on 2500 independent Monte Carlo simulations.

Data generating models: We generate n i.i.d. observations from three domains of attractions, viz $\xi > 0$, $\xi = 0$ and $\xi < 0$ for the following distributions.

1. **Case $\xi > 0$:**

$$\begin{aligned} |\text{T}|(n) : 1 - F(x) &= \int_x^\infty \frac{2\Gamma(\frac{n+1}{2})}{\sqrt{n\pi}\Gamma(\frac{n}{2})} \left(1 + \frac{w^2}{n}\right)^{-\frac{n+1}{2}} dw, \quad x > 0, \quad \xi = \frac{1}{n} \\ \text{Burr}(\eta, \lambda, \tau) : 1 - F(x) &= \left(\frac{\eta}{\eta + x^\tau}\right)^\lambda, \quad x > 0, \quad \eta, \lambda, \tau > 0, \quad \xi = \frac{1}{\lambda\tau} \end{aligned} \quad (3.1)$$

2. **Case $\xi = 0$:**

$$\begin{aligned} \text{Lognormal}(\mu, \sigma^2) : 1 - F(x) &= \int_x^\infty \frac{1}{x\sqrt{2\pi\sigma^2}} \exp\left(-\frac{(\log(x) - \mu)^2}{2\sigma^2}\right), \quad x > 0 \\ |\text{N}|(\mu, \sigma^2) : 1 - F(x) &= \int_x^\infty \frac{1}{\sqrt{2\pi\sigma^2}} \exp\left(-\frac{(x - \mu)^2}{2\sigma^2}\right) \\ \text{Weibull}(\lambda, \tau) : 1 - F(x) &= \exp(-\lambda x^\tau), \quad x > 0, \quad \lambda > 0, \tau \geq 0 \end{aligned} \quad (3.2)$$

3. **Case $\xi < 0$:**

$$\begin{aligned} \text{Beta}(p, q) : 1 - F\left(x_+ - \frac{1}{x}\right) &= \int_{1-\frac{1}{x}}^1 \frac{\Gamma(p+q)(1-u)^{q-1}}{\Gamma(p)\Gamma(q)u^{1-p}} du, \quad x > 1, p, q > 0, \quad \xi = -\frac{1}{q} \\ \text{Reverse Burr}(\eta, \lambda, \tau) : 1 - F\left(x_+ - \frac{1}{x}\right) &= \left(\frac{\eta}{\eta + x^\tau}\right)^\lambda, \quad x > 0, \eta, \lambda, \tau > 0, \quad \xi = -\frac{1}{\lambda\tau} \end{aligned} \quad (3.3)$$

The performance of the DAST algorithm for the Fréchet domain of attraction, i.e. $\xi > 0$, is discussed in section 3.1. In sections 3.2 and 3.3, we discuss the performance under Gumbel ($\xi = 0$) and reverse-Weibull ($\xi < 0$) domains of attractions respectively.

Choice of k , k^* and k_0^* : In Appendix A.1, we study the sensitivity of the DAST algorithm with respect to the choice of k , k^* and k_0^* . Both k and k^* in a neighborhood of k^{opt} where k^{opt} is given by

$$k^{\text{opt}} = \underset{k}{\operatorname{argmin}} \operatorname{Var}(GH_k) \quad (3.4)$$

Thus, k^{opt} is the optimal k at which the generalized Hill, GH_k (see (1.6)) attains the minimal variance. This k^{opt} is empirically estimated using monte carlo simulations.

Sensitivity analysis showed that choosing k_0^* as:

$$k_0^* = ck^* \frac{1}{3} \quad (3.5)$$

for $c \in (5, 10)$ works well in practice.

Outlier Scenarios: In Sections 3.1, 3.2 and 3.3, outliers are introduced in the extreme observations of the data where the top- k_0 order statistics are perturbed as follows:

$$\textit{Exponentiated Outliers} : X_{(n-i+1,n)} := X_{(n-k_0,n)} \left(\frac{X_{(n-i+1,n)}}{X_{(n-k_0,n)}} \right)^L, \quad i = 1, \dots, k_0. \quad (3.6)$$

$$\textit{Scaled Outliers} : X_{(n-i+1,n)} := X_{(n-k_0,n)} + C(X_{(n-i+1,n)} - X_{(n-k_0,n)}), \quad i = 1, \dots, k_0. \quad (3.7)$$

Note, the number of outliers is fixed at k_0 and the constants L and C control the intensity of the injected outliers. Whereas $L < 1$ and $C < 1$ shrinks the top order statistics, scenarios $L > 1$ and $C > 1$ inflate the top values. The case of $L = 1$ and $C = 1$ correspond to the regime of no outliers. For the above two kinds of outliers, the order of the bottom $(n - k_0)$ observations is preserved.

3.1 Case $\xi > 0$

We evaluate the performance of the DAST algorithm for the distribution models in Fréchet domain of attraction, i.e. $\xi > 0$ (see (3.1)). With $n = 1000$, we generate data from $|T|(1/\xi)$ and $\text{Burr}(1, 0.5, 2/\xi)$.

$k^* =$	$k=200$				$k=400$				$k=600$			
	200	400	600	ξ known	200	400	600	ξ known	200	400	600	ξ known
$\xi = 0.25$	0.092	0.036	0.034	0.034	0.09	0.048	0.048	0.048	0.081	0.066	0.066	0.066
$\xi = 0.5$	0.05	0.042	0.042	0.042	0.046	0.038	0.038	0.038	0.048	0.045	0.045	0.045
$\xi = 1$	0.046	0.046	0.046	0.046	0.036	0.036	0.036	0.036	0.032	0.032	0.032	0.032

$k^* =$	$k=100$				$k=200$				$k=300$			
	100	200	300	ξ known	100	200	300	ξ known	100	200	300	ξ known
$\xi = 0.25$	0.585	0.206	0.114	0.048	0.772	0.265	0.124	0.036	0.829	0.295	0.115	0.034
$\xi = 0.5$	0.231	0.063	0.048	0.048	0.382	0.04	0.03	0.03	0.456	0.039	0.03	0.03
$\xi = 1$	0.074	0.058	0.058	0.058	0.074	0.043	0.043	0.043	0.074	0.036	0.036	0.036

Table 1: Type 1 error for the DAST algorithm for $\xi > 0$ with $k_0^* = 7(k^*)^{1/3}$. *Top*: $|T|(1/\xi)$ distribution. *Bottom*: Burr(1,0.5,2/ ξ) distribution.

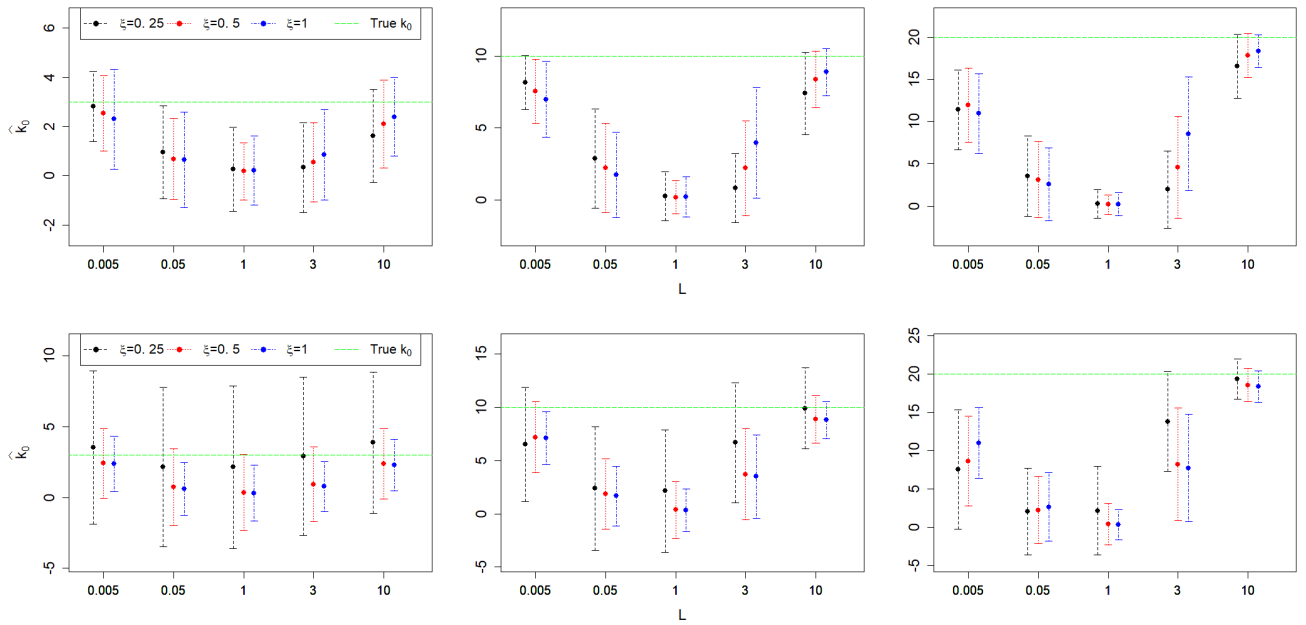


Figure 3: $E(\hat{k}_0) \pm \sqrt{\text{Var}(\hat{k}_0)}$ for exponentiated outliers, $k_0^* = 7(k^*)^{1/3}$. *Top*: $|T|(1/\xi)$, $k = k^* = 400$. *Bottom*: Burr(1,0.5,2/ ξ), $k = k^* = 200$. *Left*: $k_0 = 3$. *Middle*: $k_0 = 10$. *Right*: $k_0 = 20$.

For the set up where no outliers have been injected, i.e. $k_0 = 0$, Table 1 gives the type 1 error $\mathbb{P}(\hat{k}_0 > 0)$ for the DAST algorithm. The algorithm is fairly stable in terms of the choice of k for both Burr and $|T|$ distributions. Different values of k^* which are used in the initial estimate of ξ (see (2.7)) are indicated in the first 3 columns. On the other hand, the last column uses the true value of ξ as the initial estimate. For the $|T|$ distribution, the algorithm attains the nominal significance level at all values of ξ irrespective of the initial choice of ξ . However, for the Burr distribution, smaller values of k^* produce less reliable estimates of the initial estimate ξ especially when ξ is small. This explains the larger values of type 1 error at $\xi = 0.25$ and $k^* = 100$.

For $|T|$ and Burr distributions, Figure 3 shows the performance of the DAST for varying intensity

of the exponentiated outliers. We inject k_0 outliers according to (3.6). In this scenario, Table 4 in Appendix A.1 explores in more detail the sensitivity of the algorithm to varying choices of k and k^* .

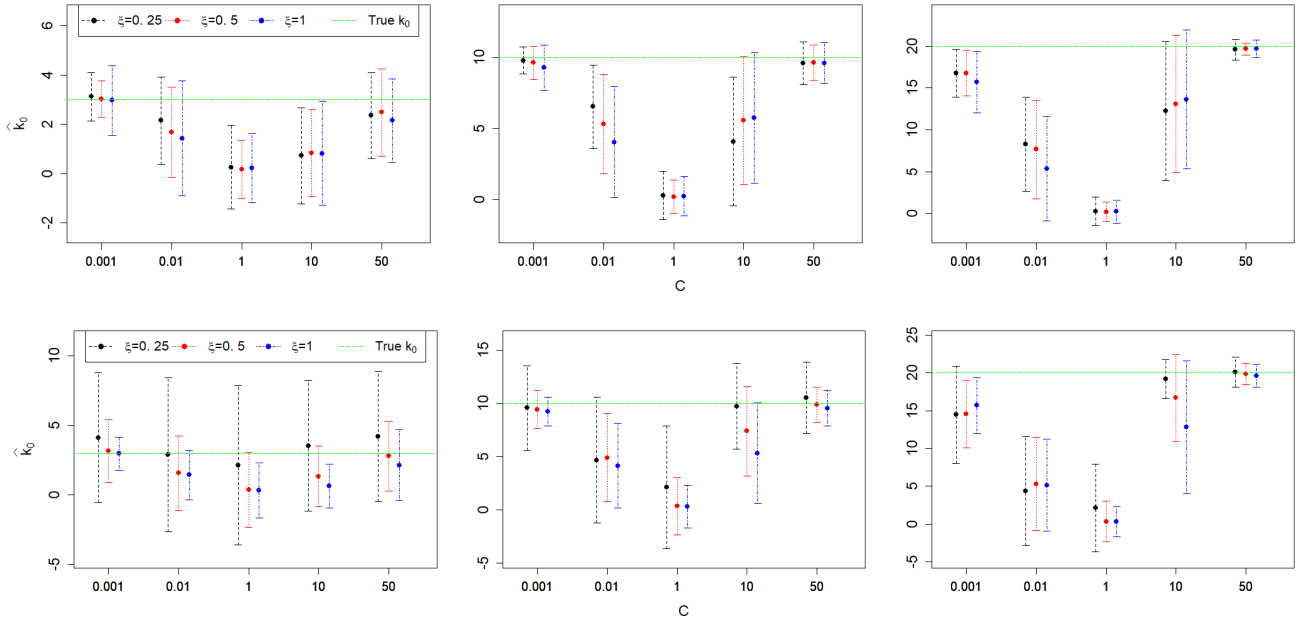


Figure 4: $E(\widehat{k}_0) \pm \sqrt{\text{Var}(\widehat{k}_0)}$ for scaled outliers, $k_0^* = 7(k^*)^{1/3}$. *Top*: $|T|(1/\xi)$, $k = k^* = 400$. *Bottom*: $\text{Burr}(1, 0.5, 2/\xi)$, $k = k^* = 200$. *Left*: $k_0 = 3$. *Middle*: $k_0 = 10$. *Right*: $k_0 = 20$.

Note, that as L deviates from 1, the performance of the algorithm improves and the best results are obtained at $L = 0.005$ and $L = 10$ for all values of k_0 . Note the improved performance of the algorithm in the region $L > 1$. This is because with $L > 1$, the outliers stand out much further from the true distribution of the data. The performance of the algorithm deteriorates with increase in k_0 . The true tail index ξ has minimal effect on the algorithm. Finally, DAST works better for the $|T|$ distribution than for the Burr distribution (observe the different scales of y-axis in top and bottom panels of Figure 3).

For $|T|$ and Burr distributions, Figure 4 shows the performance of the DAST algorithm for varying intensity of the scaled outliers. Although the performance is a bit better for the scaled than the exponentiated case, conclusions are fairly similar for both cases. The superior performance under scaled outliers is because the chosen C values produce more severe outliers. In this scenario, Table 5 in Appendix A.1 explores the sensitivity of the DAST algorithm to the choice of k and k^* .

3.2 Case $\xi = 0$

Here, with $n = 1000$, we generate data from the Gumbel domain, i.e. $\xi = 0$ (see (3.2)) viz Lognormal(0,1) (denoted by LN(0,1)), $|N|(0,1)$ and Weibull(1, τ) (denoted by W(τ)) models for $\tau = 0.5, 1, 2$.

Where no outliers have been injected, i.e. $k_0 = 0$, Table 2 gives the type 1 error, $\mathbb{P}(\widehat{k}_0 > 0)$ for the DAST algorithm. Note that when the true value of ξ is known, the algorithm is well calibrated at all values of k . However, when ξ is unknown, smaller values of k^* lead to larger values of the type 1 error. This phenomenon is more pronounced at small values of k especially for $|N|(0,1)$ and Weibull(2) distributions. This may be explained by the fact that smaller values of k^* lead to poor estimates of the initial value $\widehat{\xi}$. It is interesting to note that in a few cases DAST performs better with an estimated ξ rather than with the correct ξ (see the Weibull(2) distribution). Numerical studies showed that the generalized trimmed Hill estimator, $GH_{k_0,k}$ (see (1.6)) underestimates the tail index ξ for the given $\xi = 0$ cases. We suspect that this biased estimator of ξ perhaps facilitates easier detection of outliers.

	$k=100$				$k=150$				$k=200$			
$k^* =$	100	150	200	ξ known	100	150	200	ξ known	100	150	200	ξ known
LN(0,1)	0.204	0.074	0.048	0.036	0.27	0.069	0.044	0.034	0.325	0.072	0.044	0.036
	$k=100$				$k=200$				$k=300$			
$k^* =$	100	200	300	ξ known	100	200	300	ξ known	100	200	300	ξ known
$ N (0,1)$	0.502	0.19	0.094	0.046	0.574	0.163	0.077	0.058	0.579	0.148	0.06	0.072
	$k=100$				$k=150$				$k=200$			
$k^* =$	100	150	200	ξ known	100	150	200	ξ known	100	150	200	ξ known
W(0.5)	0.078	0.05	0.046	0.043	0.086	0.05	0.049	0.049	0.094	0.06	0.058	0.058
	$k=100$				$k=150$				$k=200$			
$k^* =$	100	150	200	ξ known	100	150	200	ξ known	100	150	200	ξ known
W(1)	0.336	0.138	0.074	0.045	0.386	0.127	0.07	0.046	0.425	0.132	0.065	0.052
	$k=200$				$k=400$				$k=600$			
$k^* =$	200	400	600	ξ known	200	400	600	ξ known	200	400	600	ξ known
W(2)	0.341	0.138	0.083	0.054	0.299	0.088	0.057	0.081	0.206	0.068	0.058	0.11

Table 2: Type 1 error for the DAST algorithm for $\xi = 0$ with $k_0^* = 7(k^*)^{1/3}$. LN denotes Lognormal(0,1) distribution and W(τ) denotes Weibull (1, τ) distribution.

For the distribution models in (3.2), Figures 5 and 6 show the performance of the DAST algorithm for varying intensity of the exponentiated and scaled outliers respectively. Tables 8 and 9 in Appendix A.1 study the sensitivity of DAST to varying choices of k and k^* . The performance of the DAST under Gumbel domain is fairly to similar to that under Fréchet domain. This is expected as the limiting distribution of the statistic $(k/k_0)^{1-\xi} - (1 - T_{k_0,k})$ is same for both $\xi > 0$ and $\xi = 0$ (see Corollary 2.3).

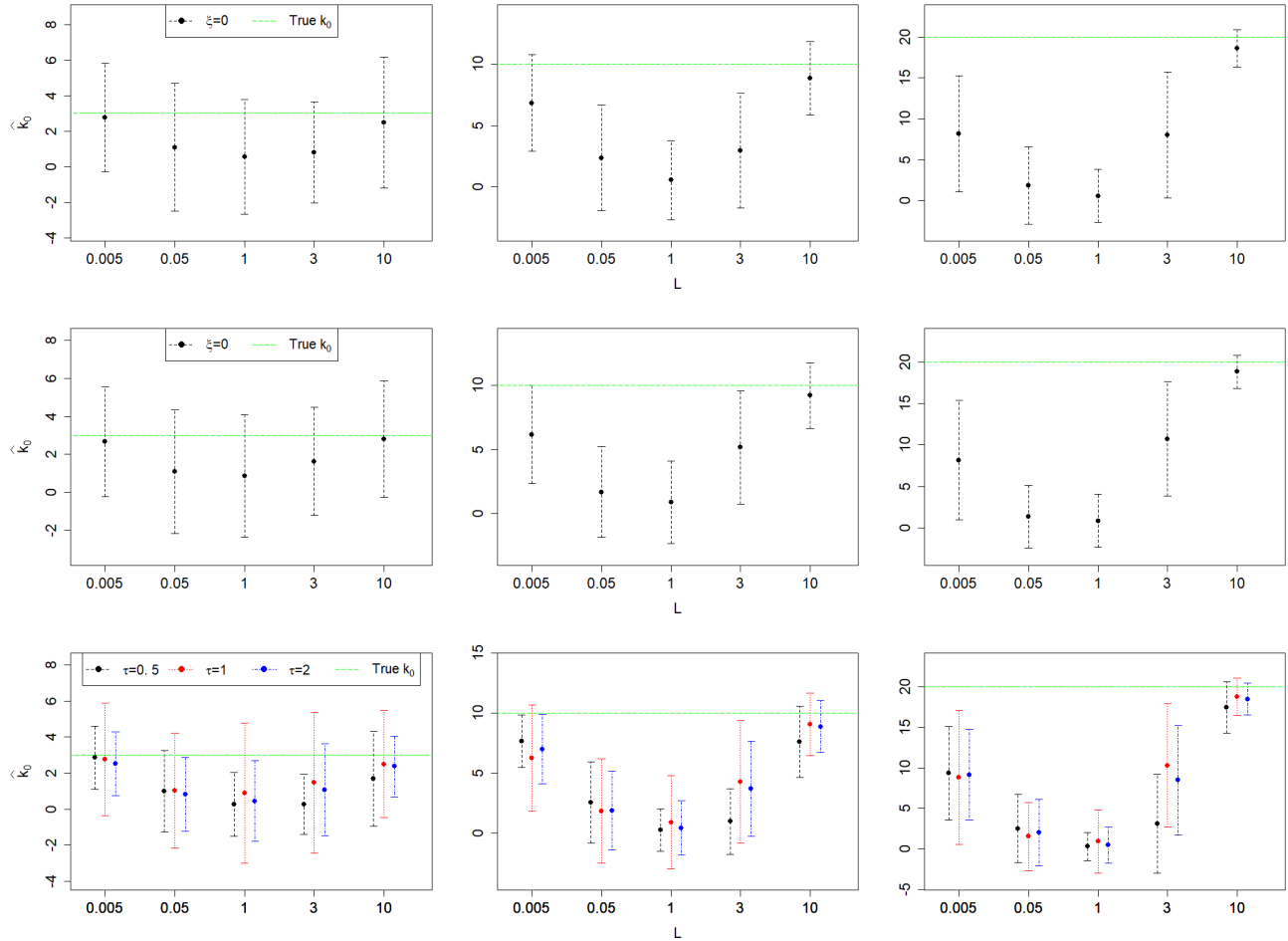


Figure 5: $E(\hat{k}_0) \pm \sqrt{\text{Var}(\hat{k}_0)}$ for exponentiated outliers, $k_0^* = 7(k^*)^{1/3}$. *Vertical:* Top: Lognormal(0,1), $k = k^* = 150$. Middle: $|N|(0,1)$, $k = k^* = 200$. Bottom: Weibull(1, τ) distribution with $k = k^* = 150, 150, 200$ for $\tau = 0.5, 1, 2$ respectively. *Horizontal:* Left: $k_0 = 3$. Middle: $k_0 = 10$. Right: $k_0 = 20$.

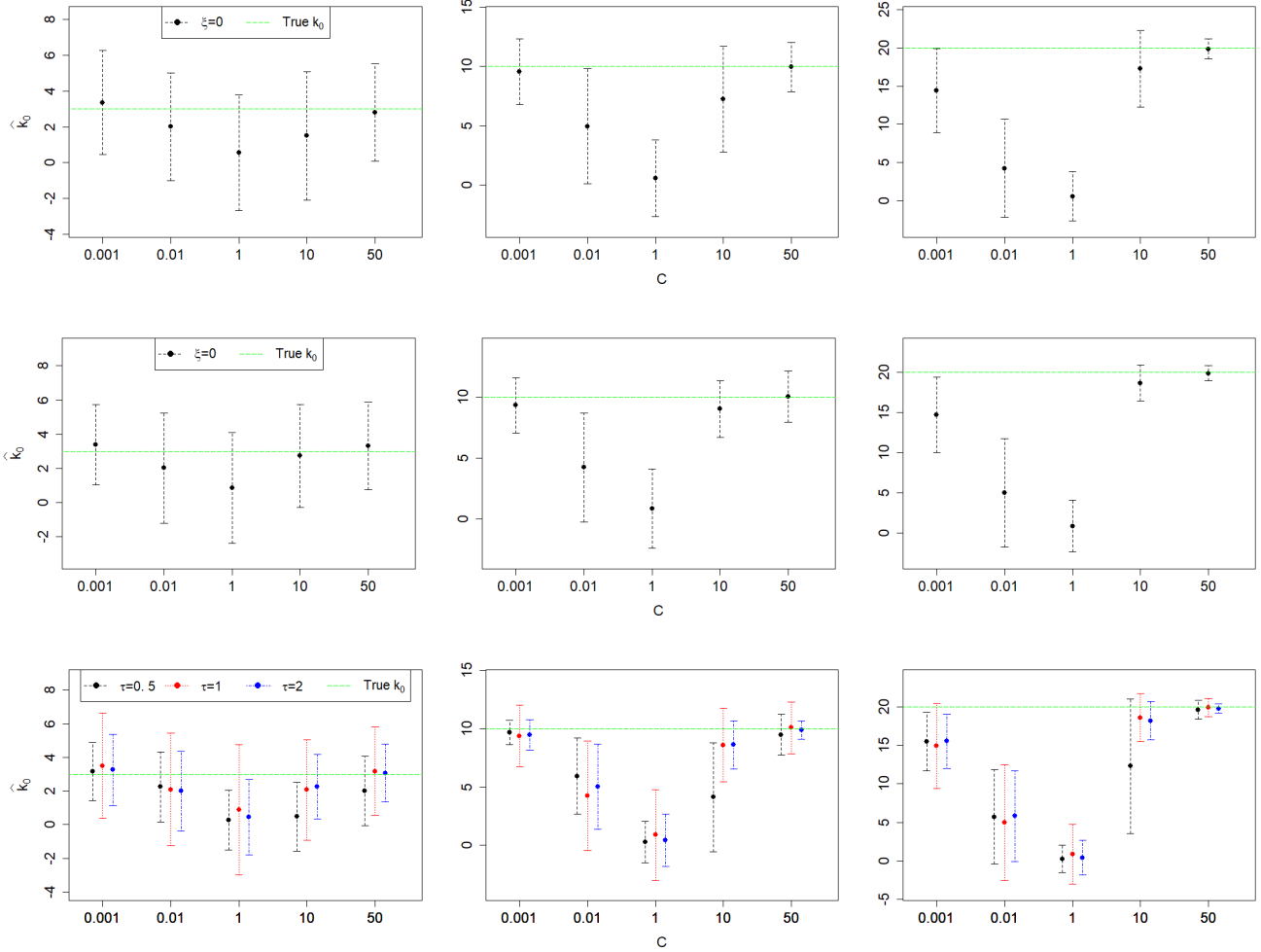


Figure 6: $E(\hat{k}_0) \pm \sqrt{\text{Var}(\hat{k}_0)}$ for scaled outliers, $k_0^* = 7(k^*)^{1/3}$. *Vertical:* *Top:* Lognormal(0,1), $k = k^* = 150$. *Middle:* $|N|(0,1)$, $k = k^* = 200$. *Bottom:* Weibull(1, τ) distribution with $k = k^* = 150, 150, 200$ for $\tau = 0.5, 1, 2$ respectively. *Horizontal:* *Left:* $k_0 = 3$. *Middle:* $k_0 = 10$. *Right:* $k_0 = 20$.

3.3 Case $\xi < 0$

Here, with $n = 1000$, we generate data from Weibull domain, i.e. $\xi < 0$ (see (3.3)) viz Beta(1,-1/ ξ) and Reverse Burr(1,0.5,-2/ ξ). The type 1 error, $\mathbb{P}(\hat{k}_0 > 0)$ when no outliers have been injected, i.e. $k_0 = 0$, is given in Table 3. Note that for $\xi = -0.25, -0.5$, the algorithm is well calibrated at all values of k when the true value of ξ is used as the initial estimate. When ξ is unknown, smaller values of k^* lead to larger type 1 errors, especially when k is taken small. For $\xi = -1$, the algorithm is not

well calibrated even if the true value of ξ is used as the initial estimate. However, $E(\widehat{k}_0)$ is quite close to zero (see Figure 7 at $L = 1$) which implies that the number of wrongly detected outliers is quite small. at $\xi = -1$ a careful analysis revealed that some of the top order statistics come very close to each other, thereby inflating the statistic $T_{k_0,k}$ (see (1.8)) at $k_0 \approx 0$, causing DAST to produce false positives.

$k^* =$	$k=100$				$k=200$				$k=300$			
	100	200	300	ξ known	100	200	300	ξ known	100	200	300	ξ known
$\xi=-0.25$	0.397	0.122	0.063	0.041	0.453	0.09	0.055	0.039	0.457	0.09	0.063	0.045
$\xi=-0.5$	0.44	0.212	0.108	0.117	0.454	0.148	0.078	0.078	0.436	0.133	0.068	0.062
$\xi=-1$	0.512	0.444	0.388	0.544	0.471	0.392	0.31	0.498	0.431	0.343	0.254	0.44

$k^* =$	$k=200$				$k=400$				$k=600$			
	200	400	600	ξ known	200	400	600	ξ known	200	400	600	ξ known
$\xi=-0.25$	0.165	0.057	0.058	0.042	0.123	0.063	0.086	0.056	0.096	0.091	0.127	0.074
$\xi=-0.5$	0.273	0.138	0.06	0.067	0.187	0.073	0.065	0.047	0.121	0.07	0.089	0.063
$\xi=-1$	0.578	0.64	0.606	0.458	0.447	0.501	0.471	0.312	0.308	0.345	0.182	0.182

Table 3: Type 1 error for the DAST algorithm for $\xi < 0$ with $k_0^* = 7(k^*)^{1/3}$. *Top*: Beta(1,1/ ξ) distribution. *Bottom*: RBurr(1,0.5,2/ ξ) distribution.

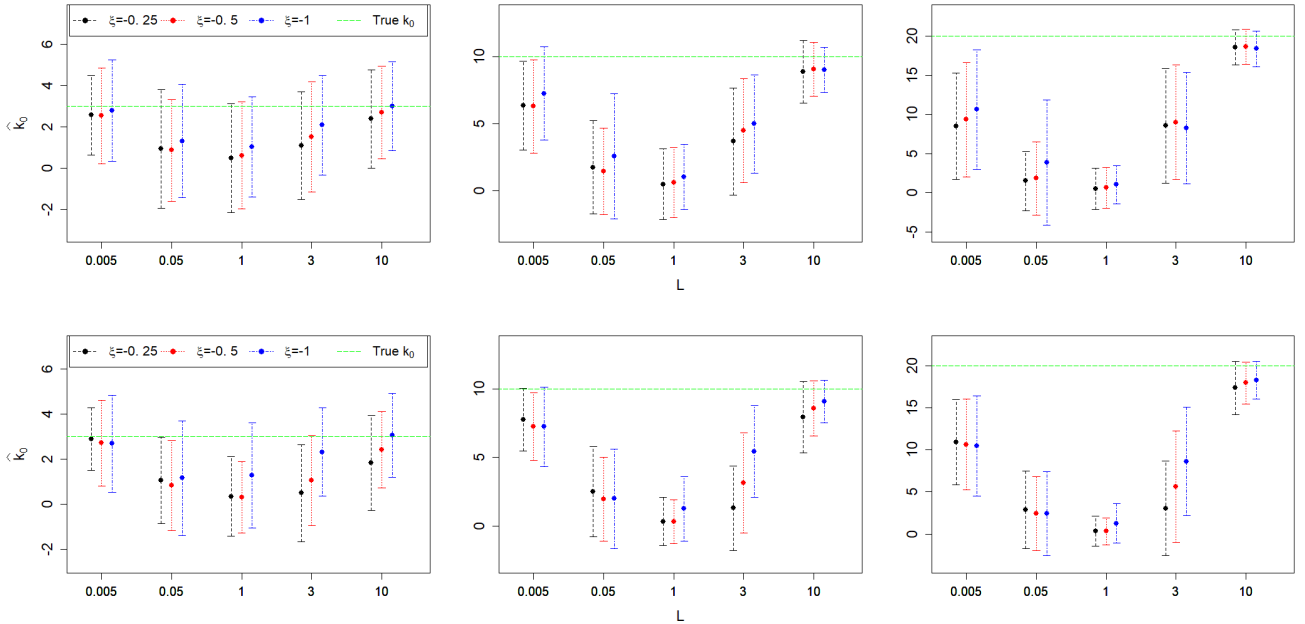


Figure 7: $E(\widehat{k}_0) \pm \sqrt{\text{Var}(\widehat{k}_0)}$ for exponentiated outliers, $k_0^* = 7(k^*)^{1/3}$. *Top*: Beta(1,-1/ ξ) distribution. *Bottom*: Reverse Burr(1,0.5,-2/ ξ) distribution. *Left*: $k_0 = 3$. *Middle*: $k_0 = 10$. *Right*: $k_0 = 20$.

For the distribution models in (3.3), Figures 7 and 8 show the performance of the DAST for varying intensity of exponentiated and scaled outliers respectively. Tables 6 and 7 in Appendix A.1 exhibit the sensitivity of the algorithm to varying choices of k and k^* . The performance of DAST improves on both sides of $L = 1$ (case of no outliers) and has greater accuracy at smaller values of k_0 . Again, the conclusions are fairly similar to those obtained in the $\xi \geq 0$ which suggests that the DAST can adapt itself easily to changing domains of attraction. Since the performance of the DAST for $\xi \leq 0$ matches that of $\xi > 0$ (see Table 4, 8 and 6) the proposed algorithm appears to be quite ubiquitous.

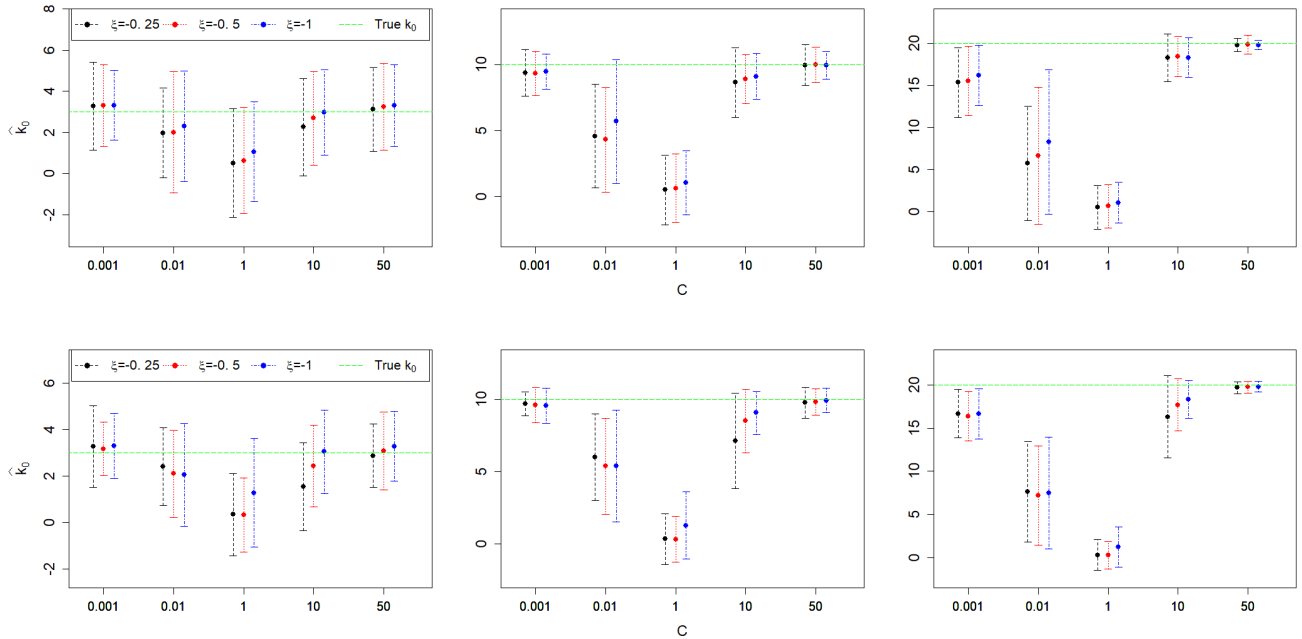


Figure 8: $E(\widehat{k}_0) \pm \sqrt{\text{Var}(\widehat{k}_0)}$ for scaled outliers, $k_0^* = 7(k^*)^{1/3}$. *Top*: Beta(1, -1/ξ), $k = k^* = 200$. *Bottom*: Reverse Burr(1, 0.5, -2/ξ), $k = k^* = 400$. *Left*: $k_0 = 3$. *Middle*: $k_0 = 10$. *Right*: $k_0 = 20$.

4 Case Studies

In this section, we apply the DAST algorithm for detection of outliers for some cases that exhibit some deviating data at one or both tails, and that appear to belong to different max-domains. The parameters a and q are set at 1.2 and 0.05. For breaking ties, the data are dithered by adding a small uniform noise from the uniform $U(-0.01, 0.01)$ distribution. In each example we take $k = k^*$. In practice, the choice of k and k^* in the neighborhood of k^{opt} as discussed/used in the section 3 (see (3.4)) is not directly applicable given that k^{opt} is not known. We propose to consider appropriate QQ-plots or the generalized QQ-plot in general, and choose $k = k^*$ around the point where a stable

tail behavior starts to kick in. This is illustrated in this section in Figures 13 left, 15 left, 11 right, and 16 right with linear fits based solely on the top $k = k^*$ observations, as used in the DAST algorithm.

4.1 French precipitation data

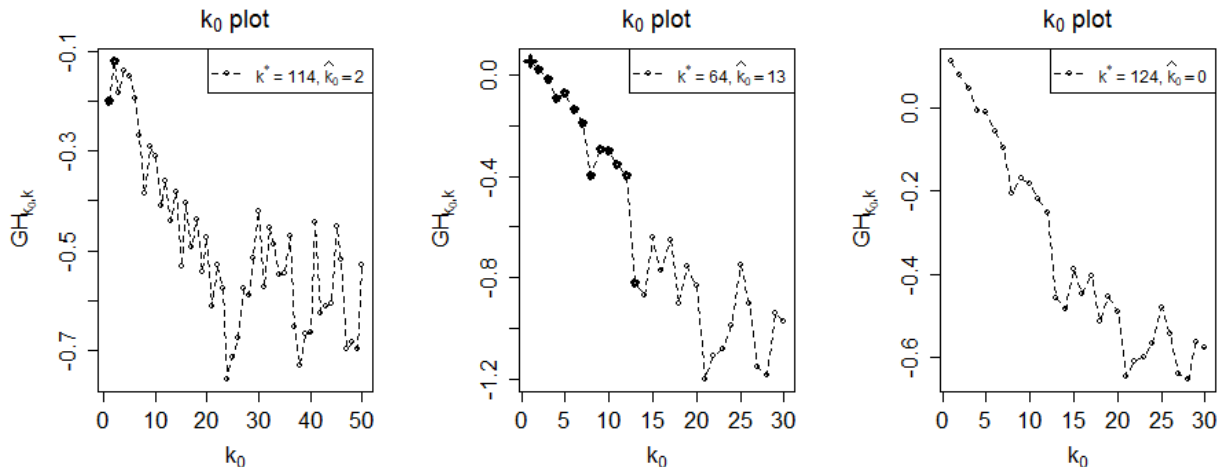


Figure 9: *French precipitation* data. *Left*: Diagnostic k_0 plot for Chamonix with $k = k^* = 114$. *Middle*: Diagnostic k_0 plot of Uzein station with $k = k^* = 64$. *Right*: Diagnostic k_0 plot of Uzein station with $k = k^* = 124$.

Concerning *the French precipitation* data discussed in section 1, we here show the diagnostic k_0 plots for both the Chamonix and Uzein stations. For the Chamonix station the top two observations exhibit a downward trend in the diagnostic k_0 plot in comparison with the remaining points. Concentrating on the top outliers only, for the Uzein station with $V = 2$, $k_0^* = 20$ and $k = k^* = 64$ we obtain 13 outliers with the largest data value being indicated separately. For $V = 2$, $k_0^* = 20$, if one chooses $k = k^* = 124$, no outliers are obtained. The sensitivity to the choice of k can be explained by the Pareto QQ-plot of Figure 2 which shows that Pareto behavior sets in around $k = k^* \leq 64$.

4.2 Toxicity data set

The *Toxicity* data set from <https://archive.ics.uci.edu/ml/datasets/QSAR+fish+toxicity> was used to develop regression models for the prediction of acute aquatic toxicity towards the Pimephales promelas. We concentrate on the LC50 count, a chemical responsible for 50% of the deaths in the fish population (see *Cassotti et al. (2015)*). Note that the classical boxplot identifies top 11 outliers whereas the tail-adjusted boxplot identifies none. This example shows an EVI $\xi \leq 0$, which is confirmed by the generalized QQ-plot in the right panel in Figure 11, which is non-increasing at the right hand side.

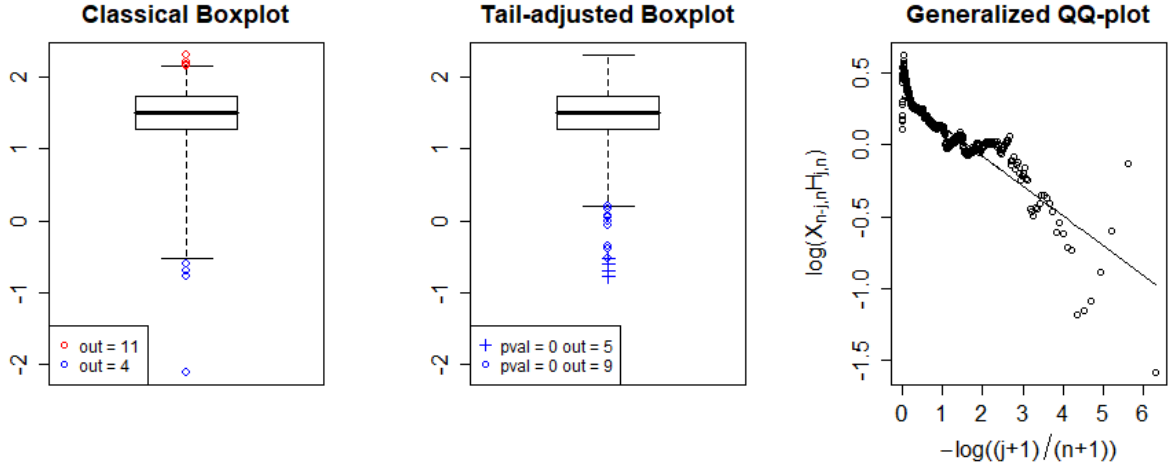


Figure 10: *Toxicity* data. *Left*: Classical boxplot. *Right*: Tail-adjusted boxplot. *Right*: Generalized QQ-Plot.

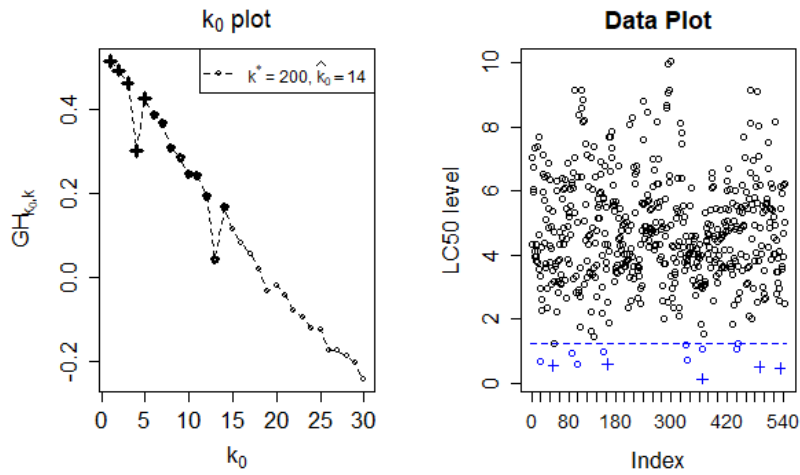


Figure 11: *Toxicity* data set. *Left*: Diagnostic k_0 plot for the left tail. *Right*: Time plot. The extreme outliers and moderate outliers are marked with + and \circ respectively.

However, a more interesting phenomenon occurs in the lower tails where the classical boxplot identifies 4 bottom outliers in contrast to 14 bottom outliers of the tail-adjusted boxplot. Using the DAST algorithm for the bottom tail with $V = 2$, $k_0^* = 30$, $k = k^* = 200$, the 14 bottom outliers are split into two regimes with 5 extreme and 9 moderate outliers. Indeed, the diagnostic k_0 plot for the bottom tail in Figure 11 shows that there are two change points at $k_0 = 5$ and $k_0 = 14$ respectively. The right panel of Figure 11 displays the time plot which indicates these 14 outliers for the bottom

tail.

4.3 French fire claims data set

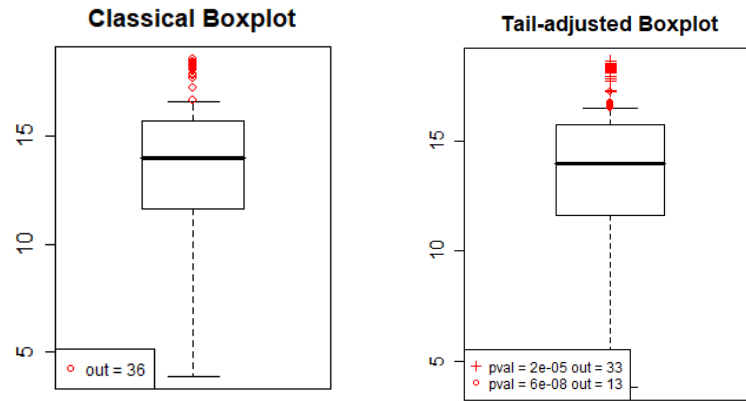


Figure 12: *Fire claim* data set. *Left*: Classical boxplot. *Right*: Tail-adjusted boxplot.

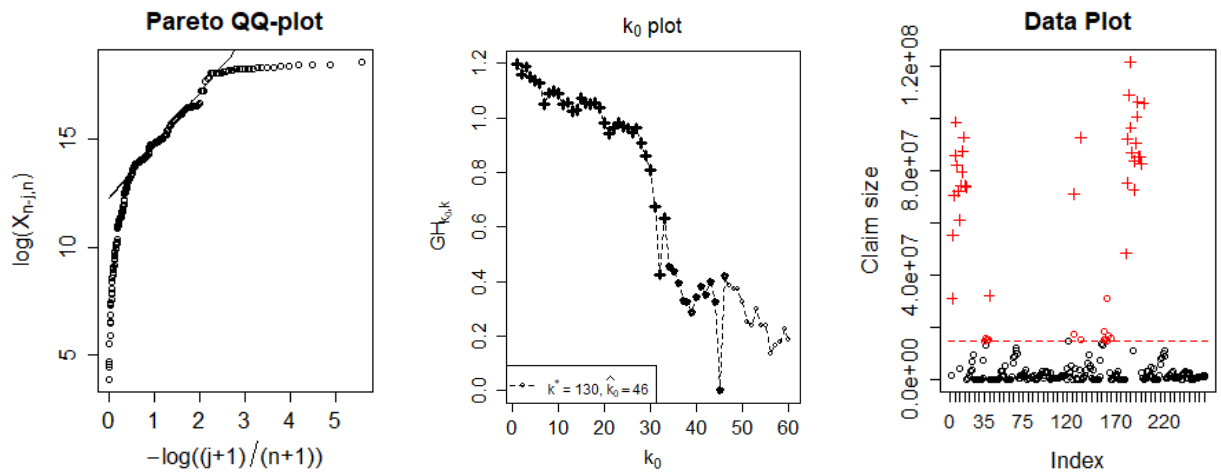


Figure 13: *Fire claim* data set. *Left*: Pareto QQ-plot. *Middle*: Diagnostic k_0 plot for the right hand tail. *Right*: Data plot. The extreme outliers and moderate outliers are marked with + and o.

The *Fire Claim* data set involves $n = 261$ claim settlements issued by a private insurer in France during the time period 1996-2006 available from <http://cas.uqam.ca/pub/R/web/CASdatasets-manual>.

pdf. This data set was already analyzed for outliers in *Bhattacharya et al. (2019)*. We here concentrate on the right tail only. The Pareto QQ-plot in Figure 13 has an apparent linear trend, up to a top group of data which exhibit less spread than the data below. Hence a different regime is present in the top data. This often appears in non-life insurance claim data due to tightened claim inspection and management with extreme claims. The boxplots are given on the log-scale in Figure 12, and the classical boxplot shows 36 top outliers.

For identifying the top outliers, the parameters of the algorithm are chosen as $V = 2$, $k_0^* = 40$, $k = k^* = 130$. Then the algorithm returns a set of $\hat{k}_0 = 33$ most extreme outliers and another group of 13 outliers which can also be noticed from the diagnostic k_0 plot with break points around positions 33 and 46. Also the Pareto QQ-plot shows some intermediate data which deviate from the linear pattern below the level $\log x = 16.5$ on the vertical scale. The top 33 outliers were already detected in *Bhattacharya et al. (2019)*.

4.4 Condroz data set

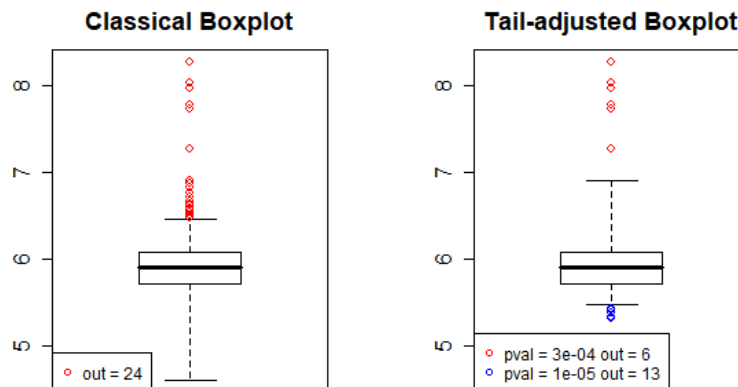


Figure 14: *Condroz* data set. *Left*: Classical boxplot. *Right*: Tail-adjusted boxplot.

The *Condroz* data set with calcium content measurements together with the pH level of soil samples in the Condroz region of Belgium was discussed in detail in *Goegebeur et al. (2005)*, and has been analyzed for outliers in *Beirlant et al. (1996)*, *Vandewalle et al. (2007)*, *Hubert and Vandervieren (2008)* and *Bhattacharya et al. (2019)*. As in these references we consider the conditional distribution of the calcium content for pH levels lying between 7-7.5 leading to $n = 420$ data values. All authors put this example in the Fréchet domain ($\xi > 0$), which is confirmed by the Pareto QQ-plot in the left panel in Figure 15 overall approximately exhibiting a linear pattern (see *Beirlant et al. (1996)*) except for the top 6 values that jump out. These outliers appeared to be measurements from communities

at the boundary of the Condroz region and hence can be considered to be sampled from another distribution (cfr. *Hubert and Vandervieren (2008)*). In *Hubert and Vandervieren (2008)* the adjusted boxplot based on robust skewness measurement shows 12 outliers.

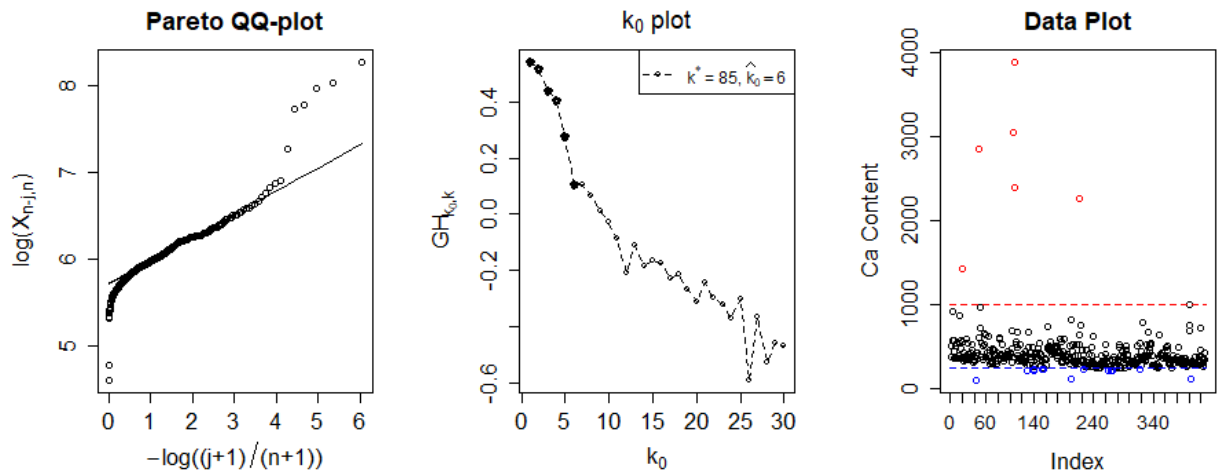


Figure 15: *Condroz* data set. *Left*: Pareto QQ-Plot. *Middle*: Diagnostic k_0 plot for the right hand tail. *Right*: Data plot.

The classical and tail-adjusted boxplots are given in Figure 14 on the log scale. For identifying both top and bottom outliers, the parameters of the algorithm are chosen as $V = 1$, $k_0^* = 30$, $k = k^* = 85$. As expected for a heavy tailed distribution, the classical boxplot indicates a high number of 24 outliers, while the tail-adjusted boxplot shows the 6 outliers corresponding with a visual inspection of the Pareto QQ-plot. This is also in consensus with the findings of *Bhattacharya et al. (2019)* where the problem of outlier identification in the heavy tailed regime ($\xi > 0$) was already discussed. Additionally, 13 left tail outliers are identified in the tail-adjusted boxplot in contrast to the classical boxplot which identifies none. The middle panel of Figure 15 contains the diagnostic k_0 plot for the right tail which shows a change point around the point $k_0 = 6$ for different values of k . The data plot is given in the right panel in Figure 15 with indication of the identified outliers in the upper and lower tails.

4.5 Air data set

The *Air Quality* data set obtained from the New York State Department of Conservation (ozone data) and the National Weather Service (meteorological data) is available at <https://stat.ethz.ch/R-manual/R-devel/library/datasets/html/airquality.html>. It contains wind speeds (in miles per hour) for New York, May to September 1973, see *Chambers and Hastie (1992)*. For this case the generalized QQ-plot shows a clear downward trend leading to $\xi < 0$ for the right tail. Here also the boxplots are given on the log scale. For identifying both top and bottom outliers, the parameters of

the DAST algorithm are chosen as $V = 1$, $k = 76$, $k^* = 76$, $k_0^* = 25$. Both the classical boxplot and tail-adjusted boxplot report 3 top outliers. In *Hubert and Vandervieren (2008)* also 3 top outliers were found using a measure of skewness. The tail-adjusted boxplot however identifies 24 bottom outliers, none of which were detected by the classical boxplot.

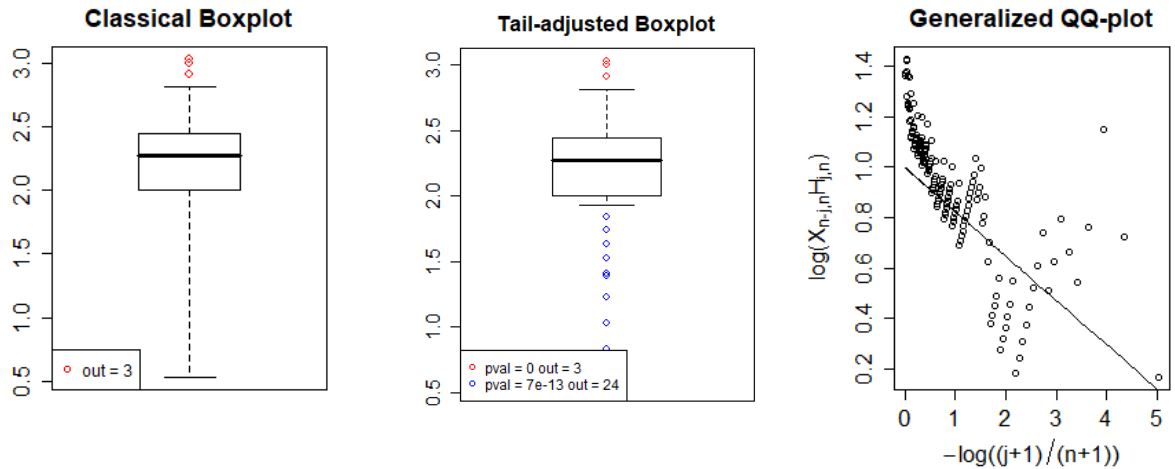


Figure 16: *Air quality* data set. *Left:* Classical boxplot. *Middle:* Tail-adjusted boxplot. *Right:* Generalized QQ-plot.

5 Conclusion

In this paper we provided a testing procedure for outlier detection based on extreme value methodology. The test statistic is based on the deviations of trimmed Hill statistics when trimming consecutive extreme data points. While the Hill estimator is only a consistent estimator in case of a positive extreme value index, we show that this statistic is still useful for outlier detection in all max-domains of attraction. As a practical consequence a tail-adjusted boxplot is proposed, allowing to indicate possible outliers depending on the tail heaviness of the underlying distribution.

References

- Beirlant, J., P. Vynckier, and J. Teugels (1996), Tail index estimation, Pareto quantile plots, and regression diagnostics, *Journal of the American Statistical Association*, 91(436), 1659–1667.
- Beirlant, J., Y. Goegebeur, J. Segers, and J. Teugels (2004), *Statistics of Extremes: Theory and Applications*, Wiley Series in Probability and Statistics, Wiley.

- Bernard, E., P. Naveau, M. Vrac, and O. Mestre (2013), Clustering of maxima: Spatial dependencies among heavy rainfall in france, *Journal of Climate*, *26*(20), 7929–7937, doi:10.1175/JCLI-D-12-00836.1.
- Bhattacharya, S., M. Kallitsis, and S. Stoev (2019), Data-adaptive trimming of the Hill estimator and detection of outliers in the extremes of heavy-tailed data, *Electronic Journal of Statistics*, *13*(1), 1872–1925, doi:10.1214/19-EJS1561.
- Cassotti, M., D. T. R. M., Ballabio, and V. Consonni (2015), A similarity-based QSAR model for predicting acute toxicity towards the fathead minnow (pimephales promelas), *SAR and QSAR in Environmental Research*, *26*(3), 217–243, doi:10.1080/1062936X.2015.1018938, pMID: 25780951.
- Chambers, J. M., and T. Hastie (1992), *Statistical Models in S*.
- de Haan, L., and A. Ferreira (2006), *Extreme Value Theory: An Introduction*, Springer Series in Operations Research and Financial Engineering, Springer New York.
- Goegebeur, Y., V. Planchon, J. Beirlant, and R. Oger (2005), Quality assessment of pedochemical data using extreme value methodology, *Journal od Applied Sciences*, *5*, 1092–1102.
- Hubert, M., and E. Vandervieren (2008), An adjusted boxplot for skewed distributions, *Computational Statistics and Data Analysis*, *52*(12), 5186 – 5201, doi:https://doi.org/10.1016/j.csda.2007.11.008.
- Tukey, J. W. (1977), *Exploratory Data Analysis*, Addison-Wesley.
- Vandewalle, B., J. Beirlant, A. Christmann, and M. Hubert (2007), A robust estimator for the tail index of Pareto-type distributions, *Computational Statistics and Data Analysis*, *51*(12), 6252 – 6268, doi:https://doi.org/10.1016/j.csda.2007.01.003.

Appendix

A.1. Further Simulation Results

We report $E(\hat{k}_0) \pm \sqrt{\text{Var}(\hat{k}_0)}$ as obtained by the DAST. The parameters are set at $V = 1$, $a = 1.2$ and $q = 0.05$. Top row corresponds to ξ known and bottom row corresponds to ξ estimated according to section 2.2 for varying k and k^* and $k_0^* = 7(k^*)^{1/3}$.

L	$k=200$			$k=400$			$k=600$		
	$k^*=200$	$k^*=400$	$k^*=600$	$k^*=200$	$k^*=400$	$k^*=600$	$k^*=200$	$k^*=400$	$k^*=600$
0.005	7.1 ± 2.5	7.1 ± 2.5	7.1 ± 2.5	7.5 ± 2.2	7.5 ± 2.2	7.5 ± 2.2	8.1 ± 1.9	8.1 ± 1.9	8.1 ± 1.9
	7 ± 3	7.1 ± 2.5	7.1 ± 2.5	7.5 ± 2.6	7.5 ± 2.2	7.5 ± 2.2	8 ± 2	8.1 ± 1.9	8.1 ± 1.9
0.05	1.8 ± 3	1.8 ± 3	1.8 ± 3	2.2 ± 3.1	2.2 ± 3.1	2.2 ± 3.1	2.8 ± 3.4	2.8 ± 3.4	2.8 ± 3.4
	2 ± 3.6	1.9 ± 3.1	1.8 ± 3	2.2 ± 3.2	2.2 ± 3.1	2.2 ± 3.1	2.7 ± 3.4	2.8 ± 3.4	2.8 ± 3.4
1	0.2 ± 1.5	0.2 ± 1.5	0.2 ± 1.5	0.2 ± 1.2	0.2 ± 1.2	0.2 ± 1.2	0.2 ± 1.5	0.2 ± 1.5	0.2 ± 1.5
	0.3 ± 2.2	0.2 ± 1.5	0.2 ± 1.5	0.2 ± 1.4	0.2 ± 1.2	0.2 ± 1.2	0.2 ± 1.5	0.2 ± 1.5	0.2 ± 1.5
3	3.3 ± 3.8	3.3 ± 3.8	3.3 ± 3.8	2.2 ± 3.3	2.2 ± 3.3	2.2 ± 3.3	1.1 ± 2.6	1.1 ± 2.6	1.1 ± 2.6
	3.5 ± 4.1	3.4 ± 3.8	3.3 ± 3.8	2.3 ± 3.5	2.2 ± 3.3	2.2 ± 3.3	1.2 ± 2.7	1.1 ± 2.6	1.1 ± 2.6
10	8.8 ± 1.7	8.8 ± 1.7	8.8 ± 1.7	8.4 ± 2	8.4 ± 2	8.4 ± 2	7.7 ± 2.5	7.7 ± 2.5	7.7 ± 2.5
	8.9 ± 2.3	8.8 ± 1.7	8.8 ± 1.7	8.5 ± 2.2	8.4 ± 2	8.4 ± 2	7.7 ± 2.7	7.7 ± 2.5	7.7 ± 2.5
30	9.8 ± 1.1	9.8 ± 1.1	9.8 ± 1.1	9.7 ± 1.1	9.7 ± 1.1	9.7 ± 1.1	9.5 ± 1.5	9.5 ± 1.5	9.5 ± 1.5
	9.9 ± 2.1	9.8 ± 1.1	9.8 ± 1.1	9.7 ± 1.6	9.7 ± 1.1	9.7 ± 1.1	9.6 ± 1.7	9.5 ± 1.5	9.5 ± 1.5

L	$k=100$			$k=200$			$k=300$		
	$k^*=100$	$k^*=200$	$k^*=300$	$k^*=100$	$k^*=200$	$k^*=300$	$k^*=100$	$k^*=200$	$k^*=300$
0.005	7.2 ± 4.2	7.2 ± 4.2	7.2 ± 4.2	7.2 ± 2.7	7.2 ± 2.7	7.2 ± 2.7	7.4 ± 2.6	7.4 ± 2.6	7.4 ± 2.6
	6.6 ± 6.3	7.2 ± 4.6	7.2 ± 4.2	7.3 ± 7.4	7.2 ± 3.3	7.2 ± 2.8	8.2 ± 8.3	7.3 ± 2.8	7.4 ± 2.6
0.05	2 ± 4.3	2 ± 4.3	2 ± 4.3	1.8 ± 3	1.8 ± 3	1.8 ± 3	1.9 ± 3.1	1.9 ± 3.1	1.9 ± 3.1
	2.7 ± 6.5	2.1 ± 4.7	2 ± 4.3	3.6 ± 7.8	1.9 ± 3.3	1.8 ± 3	4.9 ± 9.4	2 ± 3.3	1.9 ± 3.1
1	0.6 ± 4.1	0.6 ± 4.1	0.6 ± 4.1	0.2 ± 1.8	0.2 ± 1.8	0.2 ± 1.8	0.2 ± 1.6	0.2 ± 1.6	0.2 ± 1.6
	2.3 ± 6.7	0.9 ± 4.9	0.7 ± 4.2	3.8 ± 8	0.4 ± 2.7	0.2 ± 1.8	5.1 ± 9.4	0.3 ± 2.2	0.2 ± 1.8
3	4.2 ± 4.8	4.2 ± 4.8	4.2 ± 4.8	3.6 ± 4	3.6 ± 4	3.6 ± 4	2.9 ± 3.6	2.9 ± 3.6	2.9 ± 3.6
	6.4 ± 6.5	4.3 ± 5.1	4.2 ± 4.8	7.9 ± 7.7	3.7 ± 4.3	3.6 ± 4.1	8.7 ± 8.5	3.1 ± 4.3	3 ± 3.8
10	9.2 ± 3.2	9.2 ± 3.2	9.2 ± 3.2	8.8 ± 1.8	8.8 ± 1.8	8.8 ± 1.8	8.6 ± 1.9	8.6 ± 1.9	8.6 ± 1.9
	10.1 ± 4.7	9.3 ± 3.6	9.2 ± 3.2	10.7 ± 5.4	8.9 ± 2.3	8.8 ± 1.9	11.5 ± 6.7	8.7 ± 2	8.6 ± 1.9
30	10 ± 2.5	10 ± 2.5	10 ± 2.5	9.8 ± 1.1	9.8 ± 1.1	9.8 ± 1.1	9.7 ± 1	9.7 ± 1	9.7 ± 1
	10.7 ± 4.4	10.2 ± 3.3	10 ± 2.7	11.2 ± 5.1	9.8 ± 1.2	9.8 ± 1.1	11.9 ± 6.1	9.8 ± 1.4	9.7 ± 1

Table 4: $k_0 = 10$ exponentiated outliers. *Top*: $|T|(1/0.5)$. *Bottom*: $\text{Burr}(1,0.5,1/0.5)$.

C	$k=200$			$k=400$			$k=600$		
	$k^*=200$	$k^*=400$	$k^*=600$	$k^*=200$	$k^*=400$	$k^*=600$	$k^*=200$	$k^*=400$	$k^*=600$
0.001	9.5 ± 1.3	9.5 ± 1.3	9.5 ± 1.3	9.6 ± 1.2	9.6 ± 1.2	9.6 ± 1.2	9.8 ± 1.1	9.8 ± 1.1	9.8 ± 1.1
	9.5 ± 1.6	9.5 ± 1.3	9.5 ± 1.3	9.6 ± 1.4	9.6 ± 1.2	9.6 ± 1.2	9.8 ± 1.1	9.8 ± 1.1	9.8 ± 1.1
0.01	4.6 ± 3.6	4.6 ± 3.6	4.6 ± 3.6	5.3 ± 3.5	5.3 ± 3.5	5.3 ± 3.5	6.1 ± 3.3	6.1 ± 3.3	6.1 ± 3.3
	4.7 ± 3.9	4.6 ± 3.6	4.6 ± 3.6	5.3 ± 3.7	5.3 ± 3.5	5.3 ± 3.5	6 ± 3.3	6.1 ± 3.3	6.1 ± 3.3
1	0.2 ± 1.5	0.2 ± 1.5	0.2 ± 1.5	0.2 ± 1.2	0.2 ± 1.2	0.2 ± 1.2	0.2 ± 1.5	0.2 ± 1.5	0.2 ± 1.5
	0.3 ± 2.2	0.2 ± 1.5	0.2 ± 1.5	0.2 ± 1.4	0.2 ± 1.2	0.2 ± 1.2	0.2 ± 1.5	0.2 ± 1.5	0.2 ± 1.5
10	7.1 ± 3.9	7.1 ± 3.9	7.1 ± 3.9	5.5 ± 4.5	5.5 ± 4.5	5.5 ± 4.5	3.3 ± 4.5	3.3 ± 4.5	3.3 ± 4.5
	7.3 ± 4.2	7.1 ± 3.9	7.1 ± 3.9	5.7 ± 4.6	5.5 ± 4.5	5.5 ± 4.5	3.3 ± 4.5	3.3 ± 4.5	3.3 ± 4.5
50	9.8 ± 1	9.8 ± 1	9.8 ± 1	9.6 ± 1.2	9.6 ± 1.2	9.6 ± 1.2	9.2 ± 2	9.2 ± 2	9.2 ± 2
	9.8 ± 1.4	9.8 ± 1	9.8 ± 1	9.7 ± 1.4	9.6 ± 1.2	9.6 ± 1.2	9.3 ± 2	9.2 ± 2	9.2 ± 2
200	10 ± 0.5	10 ± 0.5	10 ± 0.5	10 ± 0.5	10 ± 0.5	10 ± 0.5	9.9 ± 0.7	9.9 ± 0.7	9.9 ± 0.7
	10.1 ± 1.6	10 ± 0.5	10 ± 0.5	10 ± 1.1	10 ± 0.5	10 ± 0.5	9.9 ± 0.7	9.9 ± 0.7	9.9 ± 0.7

C	$k=100$			$k=200$			$k=300$		
	$k^*=100$	$k^*=200$	$k^*=300$	$k^*=100$	$k^*=200$	$k^*=300$	$k^*=100$	$k^*=200$	$k^*=300$
0.001	9.5 ± 3	9.5 ± 3	9.5 ± 3	9.4 ± 1.3	9.4 ± 1.3	9.4 ± 1.3	9.5 ± 1.1	9.5 ± 1.1	9.5 ± 1.1
	9.7 ± 5.2	9.6 ± 3.4	9.5 ± 3.1	10.1 ± 5.9	9.4 ± 1.8	9.4 ± 1.4	11.1 ± 7.3	9.6 ± 1.9	9.5 ± 1.1
0.01	4.7 ± 4.6	4.7 ± 4.6	4.7 ± 4.6	4.8 ± 3.7	4.8 ± 3.7	4.8 ± 3.7	5.1 ± 3.5	5.1 ± 3.5	5.1 ± 3.5
	4.7 ± 6.4	4.8 ± 5	4.7 ± 4.8	5.5 ± 7.6	4.9 ± 4.2	4.9 ± 3.9	6.6 ± 8.9	5.1 ± 3.9	5.1 ± 3.6
1	0.6 ± 4.1	0.6 ± 4.1	0.6 ± 4.1	0.2 ± 1.8	0.2 ± 1.8	0.2 ± 1.8	0.2 ± 1.6	0.2 ± 1.6	0.2 ± 1.6
	2.3 ± 6.7	0.9 ± 4.9	0.7 ± 4.2	3.8 ± 8	0.4 ± 2.7	0.2 ± 1.8	5.1 ± 9.4	0.3 ± 2.2	0.2 ± 1.8
10	7.9 ± 4.1	7.9 ± 4.1	7.9 ± 4.1	7.3 ± 3.9	7.3 ± 3.9	7.3 ± 3.9	6.6 ± 4.2	6.6 ± 4.2	6.6 ± 4.2
	9.3 ± 5.4	8.1 ± 4.6	8 ± 4.3	10 ± 6	7.4 ± 4.2	7.3 ± 3.9	10.7 ± 7.3	6.7 ± 4.2	6.6 ± 4.2
50	10 ± 2.5	10 ± 2.5	10 ± 2.5	9.8 ± 0.9	9.8 ± 0.9	9.8 ± 0.9	9.8 ± 1	9.8 ± 1	9.8 ± 1
	10.7 ± 4.2	10.2 ± 3	10.1 ± 2.7	11.3 ± 5.3	9.9 ± 1.7	9.8 ± 1.2	12 ± 6.6	9.8 ± 1.5	9.8 ± 1
200	10.2 ± 2.7	10.2 ± 2.7	10.2 ± 2.7	10 ± 1	10 ± 1	10 ± 1	10 ± 0.6	10 ± 0.6	10 ± 0.6
	10.9 ± 4.3	10.4 ± 3.2	10.2 ± 2.7	11.5 ± 5.2	10.1 ± 1.6	10 ± 1.2	12.2 ± 6.5	10 ± 1.2	10 ± 0.6

Table 5: $k_0 = 10$ scaled outliers. *Top*: $|T|(1/0.5)$. *Bottom*: $\text{Burr}(1,0.5,1/0.5)$.

L	$k=100$			$k=200$			$k=300$		
	$k^*=100$	$k^*=200$	$k^*=300$	$k^*=100$	$k^*=200$	$k^*=300$	$k^*=100$	$k^*=200$	$k^*=300$
0.005	7.2 ± 2.6	7.2 ± 2.6	7.2 ± 2.6	7.6 ± 2.2	7.6 ± 2.2	7.6 ± 2.2	7.8 ± 2.1	7.8 ± 2.1	7.8 ± 2.1
	7.5 ± 6	6.5 ± 4	6.8 ± 3.3	9.9 ± 7.7	6.3 ± 3.5	7 ± 2.8	10.8 ± 8.5	6.4 ± 3.4	7.2 ± 2.6
0.05	1.9 ± 3.2	1.9 ± 3.2	1.9 ± 3.2	2.1 ± 3.2	2.1 ± 3.2	2.1 ± 3.2	2.3 ± 3.2	2.3 ± 3.2	2.3 ± 3.2
	2.7 ± 6.2	1.8 ± 4.2	1.9 ± 3.9	4 ± 7.3	1.5 ± 3.2	1.9 ± 3.4	4.3 ± 7.6	1.5 ± 3.2	2 ± 3.2
1	0.4 ± 2.2	0.4 ± 2.2	0.4 ± 2.2	0.3 ± 1.8	0.3 ± 1.8	0.3 ± 1.8	0.3 ± 2	0.3 ± 2	0.3 ± 2
	2.2 ± 4.7	1.2 ± 4	0.6 ± 3.1	2.6 ± 5.3	0.6 ± 2.6	0.4 ± 2.1	2.6 ± 5.4	0.6 ± 2.6	0.4 ± 2.1
3	5 ± 3.5	5 ± 3.5	5 ± 3.5	4.1 ± 3.4	4.1 ± 3.4	4.1 ± 3.4	3.2 ± 3.3	3.2 ± 3.3	3.2 ± 3.3
	6.8 ± 4.4	5.4 ± 4.5	4.4 ± 4.1	6.6 ± 4.8	4.5 ± 3.9	3.3 ± 3.8	6.2 ± 5	3.8 ± 3.8	2.4 ± 3.5
10	9.1 ± 1.8	9.1 ± 1.8	9.1 ± 1.8	8.9 ± 1.6	8.9 ± 1.6	8.9 ± 1.6	8.6 ± 1.8	8.6 ± 1.8	8.6 ± 1.8
	9.7 ± 2.7	9.4 ± 2.8	9.1 ± 2.3	9.7 ± 3	9.1 ± 2	8.7 ± 2	9.7 ± 3.3	8.8 ± 2.1	8.4 ± 2.1
30	9.8 ± 1.6	9.8 ± 1.6	9.8 ± 1.6	9.7 ± 1	9.7 ± 1	9.7 ± 1	9.7 ± 1	9.7 ± 1	9.7 ± 1
	10.2 ± 2.5	10.1 ± 2.3	9.9 ± 1.9	10.3 ± 2.7	9.8 ± 1.3	9.7 ± 1.2	10.4 ± 3	9.8 ± 1.3	9.7 ± 1.1

L	$k=200$			$k=400$			$k=600$		
	$k^*=200$	$k^*=400$	$k^*=600$	$k^*=200$	$k^*=400$	$k^*=600$	$k^*=200$	$k^*=400$	$k^*=600$
0.005	7.5 ± 2.1	7.5 ± 2.1	7.5 ± 2.1	8.1 ± 1.8	8.1 ± 1.8	8.1 ± 1.8	8.7 ± 1.6	8.7 ± 1.6	8.7 ± 1.6
	6.2 ± 3.9	6.8 ± 3	7.4 ± 2.5	6.4 ± 3.5	7.2 ± 2.5	7.9 ± 2	6.8 ± 3	7.9 ± 2.2	8.5 ± 1.8
0.05	2.1 ± 3.1	2.1 ± 3.1	2.1 ± 3.1	2.6 ± 3.2	2.6 ± 3.2	2.6 ± 3.2	3.4 ± 3.4	3.4 ± 3.4	3.4 ± 3.4
	1.5 ± 3.4	1.7 ± 3.2	2 ± 3.2	1.5 ± 2.9	2 ± 3.1	2.5 ± 3.2	1.7 ± 3	2.5 ± 3.2	3.3 ± 3.5
1	0.3 ± 1.5	0.3 ± 1.5	0.3 ± 1.5	0.2 ± 1.4	0.2 ± 1.4	0.2 ± 1.4	0.4 ± 1.8	0.4 ± 1.8	0.4 ± 1.8
	1.1 ± 3.3	0.6 ± 2.3	0.3 ± 1.6	0.7 ± 2.3	0.3 ± 1.6	0.3 ± 1.8	0.5 ± 2.1	0.4 ± 1.8	0.5 ± 2.2
3	4.2 ± 3.6	4.2 ± 3.6	4.2 ± 3.6	2.3 ± 3.2	2.3 ± 3.2	2.3 ± 3.2	1 ± 2.6	1 ± 2.6	1 ± 2.6
	6 ± 4.2	5 ± 4	3.4 ± 3.8	4.6 ± 4.1	3.1 ± 3.6	1.6 ± 3.2	2.7 ± 3.7	1.5 ± 3.1	0.7 ± 2.6
10	8.9 ± 1.7	8.9 ± 1.7	8.9 ± 1.7	8.3 ± 2	8.3 ± 2	8.3 ± 2	7.2 ± 2.7	7.2 ± 2.7	7.2 ± 2.7
	9.3 ± 1.9	9 ± 1.7	8.7 ± 1.9	8.9 ± 2	8.6 ± 2	7.9 ± 2.5	8.2 ± 2.5	7.6 ± 2.7	6.5 ± 3.4
30	9.7 ± 0.8	9.7 ± 0.8	9.7 ± 0.8	9.6 ± 0.9	9.6 ± 0.9	9.6 ± 0.9	9.4 ± 1.2	9.4 ± 1.2	9.4 ± 1.2
	9.9 ± 1.5	9.8 ± 1.1	9.7 ± 0.9	9.8 ± 1.1	9.7 ± 0.9	9.5 ± 1	9.6 ± 1.1	9.5 ± 1.1	9.3 ± 1.3

Table 6: $k_0 = 10$ exponentiated outliers. *Top*: Beta(1,1/0.5). *Bottom*: Reverse Burr(1,0.5,1/0.5).

C	$k=100$			$k=200$			$k=300$		
	$k^*=100$	$k^*=200$	$k^*=300$	$k^*=100$	$k^*=200$	$k^*=300$	$k^*=100$	$k^*=200$	$k^*=300$
0.001	9.6 ± 1.8	9.6 ± 1.8	9.6 ± 1.8	9.6 ± 0.9	9.6 ± 0.9	9.6 ± 0.9	9.7 ± 1	9.7 ± 1	9.7 ± 1
	9.6 ± 3.5	9.5 ± 2.5	9.5 ± 2.1	9.8 ± 3.7	9.3 ± 1.7	9.5 ± 1.3	10.1 ± 4.3	9.4 ± 1.8	9.6 ± 1
0.01	5.4 ± 3.6	5.4 ± 3.6	5.4 ± 3.6	5.8 ± 3	5.8 ± 3	5.8 ± 3	6.2 ± 2.9	6.2 ± 2.9	6.2 ± 2.9
	6.4 ± 7	4.5 ± 4.6	4.9 ± 4	8.8 ± 8.4	4.3 ± 4	5 ± 3.5	10 ± 9.1	4.4 ± 3.8	5.3 ± 3.4
1	0.4 ± 2.2	0.4 ± 2.2	0.4 ± 2.2	0.3 ± 1.8	0.3 ± 1.8	0.3 ± 1.8	0.3 ± 2	0.3 ± 2	0.3 ± 2
	2.2 ± 4.7	1.2 ± 4	0.6 ± 3.1	2.6 ± 5.3	0.6 ± 2.6	0.4 ± 2.1	2.6 ± 5.4	0.6 ± 2.6	0.4 ± 2.1
10	9 ± 1.6	9 ± 1.6	9 ± 1.6	8.8 ± 1.6	8.8 ± 1.6	8.8 ± 1.6	8.5 ± 1.9	8.5 ± 1.9	8.5 ± 1.9
	9.6 ± 2.6	9.2 ± 2.4	8.9 ± 2	9.6 ± 3	8.9 ± 1.9	8.5 ± 2.1	9.6 ± 3.5	8.6 ± 2.1	8.2 ± 2.4
50	10 ± 1.4	10 ± 1.4	10 ± 1.4	9.9 ± 0.8	9.9 ± 0.8	9.9 ± 0.8	9.9 ± 0.8	9.9 ± 0.8	9.9 ± 0.8
	10.5 ± 3.2	10.3 ± 2.9	10.1 ± 2.4	10.5 ± 3.1	10 ± 1.4	9.9 ± 1	10.5 ± 3.2	10 ± 1.3	9.9 ± 0.8
200	10 ± 1.2	10 ± 1.2	10 ± 1.2	10 ± 0.7	10 ± 0.7	10 ± 0.7	10 ± 0.7	10 ± 0.7	10 ± 0.7
	10.4 ± 2.6	10.2 ± 2	10.1 ± 1.7	10.5 ± 2.6	10.1 ± 1.1	10 ± 1	10.5 ± 2.8	10 ± 0.9	10 ± 0.7

C	$k=200$			$k=400$			$k=600$		
	$k^*=200$	$k^*=400$	$k^*=600$	$k^*=200$	$k^*=400$	$k^*=600$	$k^*=200$	$k^*=400$	$k^*=600$
0.001	9.6 ± 1.1	9.6 ± 1.1	9.6 ± 1.1	9.8 ± 1.1	9.8 ± 1.1	9.8 ± 1.1	10 ± 1	10 ± 1	10 ± 1
	9.4 ± 2.4	9.5 ± 1.6	9.6 ± 1.3	9.4 ± 1.9	9.6 ± 1.2	9.8 ± 1.1	9.6 ± 1.4	9.8 ± 1.1	9.9 ± 1
0.01	5.8 ± 3	5.8 ± 3	5.8 ± 3	6.6 ± 2.8	6.6 ± 2.8	6.6 ± 2.8	7.4 ± 2.4	7.4 ± 2.4	7.4 ± 2.4
	4.2 ± 4.3	4.8 ± 3.6	5.6 ± 3.2	4.4 ± 4.1	5.4 ± 3.3	6.3 ± 3	4.8 ± 3.7	6.2 ± 3.1	7.1 ± 2.7
1	0.3 ± 1.5	0.3 ± 1.5	0.3 ± 1.5	0.2 ± 1.4	0.2 ± 1.4	0.2 ± 1.4	0.4 ± 1.8	0.4 ± 1.8	0.4 ± 1.8
	1.1 ± 3.3	0.6 ± 2.3	0.3 ± 1.6	0.7 ± 2.3	0.3 ± 1.6	0.3 ± 1.8	0.5 ± 2.1	0.4 ± 1.8	0.5 ± 2.2
10	8.8 ± 1.8	8.8 ± 1.8	8.8 ± 1.8	8.2 ± 2.2	8.2 ± 2.2	8.2 ± 2.2	6.9 ± 3	6.9 ± 3	6.9 ± 3
	9.4 ± 2.5	9 ± 2.2	8.7 ± 2.1	8.9 ± 2.5	8.5 ± 2.2	7.8 ± 2.8	8 ± 2.9	7.4 ± 3	6 ± 3.7
50	9.9 ± 0.9	9.9 ± 0.9	9.9 ± 0.9	9.8 ± 0.9	9.8 ± 0.9	9.8 ± 0.9	9.7 ± 1.2	9.7 ± 1.2	9.7 ± 1.2
	10.1 ± 2	10 ± 1.6	9.9 ± 1.2	10 ± 1.4	9.8 ± 0.9	9.8 ± 1	9.8 ± 1	9.8 ± 1	9.7 ± 1.3
200	10 ± 0.6	10 ± 0.6	10 ± 0.6	10 ± 0.6	10 ± 0.6	10 ± 0.6	10 ± 0.8	10 ± 0.8	10 ± 0.8
	10.1 ± 1.5	10 ± 0.9	10 ± 0.6	10.1 ± 1.1	10 ± 0.7	10 ± 0.6	10 ± 0.7	10 ± 0.7	10 ± 0.8

Table 7: $k_0 = 10$ scaled outliers. *Top*: Beta(1,1/0.5). *Bottom*: Reverse Burr(1,0.5,1/0.5).

L	$k=100$			$k=150$			$k=200$		
	$k^*=100$	$k^*=150$	$k^*=200$	$k^*=100$	$k^*=150$	$k^*=200$	$k^*=100$	$k^*=150$	$k^*=200$
0.005	7.4 ± 3.4	7.4 ± 3.4	7.4 ± 3.4	7.6 ± 2.5	7.6 ± 2.5	7.6 ± 2.5	7.7 ± 2.3	7.7 ± 2.3	7.7 ± 2.3
	6.4 ± 5.8	6.9 ± 4.6	7.3 ± 4	6.6 ± 6.2	6.8 ± 3.9	7.3 ± 2.9	6.8 ± 6.6	6.9 ± 3.9	7.5 ± 2.8
0.05	2.2 ± 3.6	2.2 ± 3.6	2.2 ± 3.6	2.3 ± 3.2	2.3 ± 3.2	2.3 ± 3.2	2.5 ± 3.2	2.5 ± 3.2	2.5 ± 3.2
	2.7 ± 6.3	2.5 ± 5	2.4 ± 4.3	2.6 ± 6.1	2.4 ± 4.3	2.4 ± 3.7	3.1 ± 6.8	2.3 ± 3.9	2.5 ± 3.6
1	0.3 ± 2.6	0.3 ± 2.6	0.3 ± 2.6	0.2 ± 1.6	0.2 ± 1.6	0.2 ± 1.6	0.2 ± 1.3	0.2 ± 1.3	0.2 ± 1.3
	1.7 ± 5.5	0.8 ± 4.1	0.5 ± 3.1	2.2 ± 6	0.6 ± 3.2	0.3 ± 2.5	2.8 ± 6.6	0.5 ± 3.1	0.3 ± 2.2
3	2.6 ± 4.5	2.6 ± 4.5	2.6 ± 4.5	1.9 ± 3.3	1.9 ± 3.3	1.9 ± 3.3	1.5 ± 3.1	1.5 ± 3.1	1.5 ± 3.1
	5.5 ± 6.1	3.5 ± 5.4	2.9 ± 5	5.9 ± 6.3	3 ± 4.7	2.1 ± 3.8	6.5 ± 7	2.8 ± 4.7	1.8 ± 3.5
10	8.7 ± 2.7	8.7 ± 2.7	8.7 ± 2.7	8.4 ± 2.2	8.4 ± 2.2	8.4 ± 2.2	8.2 ± 2.2	8.2 ± 2.2	8.2 ± 2.2
	9.8 ± 4	9.2 ± 3.7	8.9 ± 3.2	9.8 ± 4	8.8 ± 3	8.5 ± 2.6	10.1 ± 4.6	8.7 ± 2.9	8.3 ± 2.5
30	9.8 ± 2.1	9.8 ± 2.1	9.8 ± 2.1	9.7 ± 1	9.7 ± 1	9.7 ± 1	9.6 ± 1.1	9.6 ± 1.1	9.6 ± 1.1
	10.4 ± 3.5	10 ± 2.9	9.9 ± 2.5	10.5 ± 3.8	9.9 ± 2.3	9.7 ± 1.9	10.8 ± 4.4	9.8 ± 1.9	9.7 ± 1.2

L	$k=100$			$k=200$			$k=300$		
	$k^*=100$	$k^*=200$	$k^*=300$	$k^*=100$	$k^*=200$	$k^*=300$	$k^*=100$	$k^*=200$	$k^*=300$
0.005	7.8 ± 2.5	7.8 ± 2.5	7.8 ± 2.5	8.4 ± 1.8	8.4 ± 1.8	8.4 ± 1.8	8.8 ± 1.7	8.8 ± 1.7	8.8 ± 1.7
	6.8 ± 6.5	6.4 ± 4.7	6.9 ± 4.1	8.8 ± 7.6	6.2 ± 3.9	6.8 ± 3.1	9.7 ± 8.3	6.3 ± 3.9	7 ± 2.8
0.05	2.6 ± 3.3	2.6 ± 3.3	2.6 ± 3.3	3.3 ± 3.3	3.3 ± 3.3	3.3 ± 3.3	3.9 ± 3.3	3.9 ± 3.3	3.9 ± 3.3
	2.5 ± 6.2	1.9 ± 4.6	1.8 ± 4	3.3 ± 7.1	1.7 ± 3.5	1.9 ± 3.4	3.7 ± 7.8	1.7 ± 3.4	2 ± 3.1
1	0.3 ± 2.2	0.3 ± 2.2	0.3 ± 2.2	0.3 ± 1.7	0.3 ± 1.7	0.3 ± 1.7	0.4 ± 1.9	0.4 ± 1.9	0.4 ± 1.9
	3.2 ± 6.4	1.3 ± 4.7	0.7 ± 3.7	4.4 ± 7.5	0.9 ± 3.2	0.4 ± 2.4	4.8 ± 8.2	0.7 ± 2.8	0.3 ± 1.9
3	1 ± 3	1 ± 3	1 ± 3	0.4 ± 2.3	0.4 ± 2.3	0.4 ± 2.3	0.3 ± 2.3	0.3 ± 2.3	0.3 ± 2.3
	7.8 ± 5.2	5.7 ± 5.1	4.7 ± 4.8	8.4 ± 6.1	5.2 ± 4.4	3.7 ± 4.2	8.7 ± 6.9	4.4 ± 4.3	2.7 ± 3.7
10	7.9 ± 3.2	7.9 ± 3.2	7.9 ± 3.2	6.5 ± 3.5	6.5 ± 3.5	6.5 ± 3.5	5 ± 3.9	5 ± 3.9	5 ± 3.9
	10.2 ± 3.8	9.5 ± 3.2	9.2 ± 3	10.7 ± 4.6	9.2 ± 2.6	8.9 ± 2.3	10.8 ± 5	8.9 ± 2.3	8.5 ± 2.1
30	9.6 ± 1.6	9.6 ± 1.6	9.6 ± 1.6	9.4 ± 1.3	9.4 ± 1.3	9.4 ± 1.3	9.1 ± 1.6	9.1 ± 1.6	9.1 ± 1.6
	10.6 ± 3.4	10.2 ± 2.9	10 ± 2.2	11.1 ± 4.4	10 ± 1.9	9.8 ± 1.3	11.3 ± 5	9.9 ± 1.7	9.7 ± 1.3

L	$k=100$			$k=150$			$k=200$		
	$k^*=100$	$k^*=150$	$k^*=200$	$k^*=100$	$k^*=150$	$k^*=200$	$k^*=100$	$k^*=150$	$k^*=200$
0.005	7.7 ± 2.5	7.7 ± 2.5	7.7 ± 2.5	8 ± 2	8 ± 2	8 ± 2	8.2 ± 1.8	8.2 ± 1.8	8.2 ± 1.8
	6.1 ± 5.7	6.4 ± 4.8	6.8 ± 4.1	6.7 ± 6.2	6.2 ± 4.4	6.7 ± 3.4	7 ± 6.4	6.2 ± 4.2	6.9 ± 3.1
0.05	2.4 ± 3.5	2.4 ± 3.5	2.4 ± 3.5	2.6 ± 3.1	2.6 ± 3.1	2.6 ± 3.1	2.8 ± 3.2	2.8 ± 3.2	2.8 ± 3.2
	2.2 ± 5.8	2 ± 4.9	2.1 ± 4.6	2.4 ± 5.8	1.8 ± 4.3	2 ± 3.8	2.8 ± 6.7	1.8 ± 4.1	2 ± 3.5
1	0.4 ± 2.8	0.4 ± 2.8	0.4 ± 2.8	0.3 ± 1.6	0.3 ± 1.6	0.3 ± 1.6	0.3 ± 1.8	0.3 ± 1.8	0.3 ± 1.8
	2.3 ± 5.9	1.1 ± 4.7	0.7 ± 4.1	2.8 ± 6.3	0.9 ± 3.9	0.6 ± 3.4	3.3 ± 6.9	0.9 ± 3.8	0.5 ± 2.6
3	1.4 ± 3.8	1.4 ± 3.8	1.4 ± 3.8	0.9 ± 2.9	0.9 ± 2.9	0.9 ± 2.9	0.7 ± 2.7	0.7 ± 2.7	0.7 ± 2.7
	6.6 ± 6	4.7 ± 5.6	3.4 ± 5.2	6.9 ± 6.1	4.3 ± 5.1	2.8 ± 4.5	7.2 ± 6.6	4 ± 5	2.4 ± 4.1
10	8.1 ± 2.9	8.1 ± 2.9	8.1 ± 2.9	7.5 ± 2.9	7.5 ± 2.9	7.5 ± 2.9	7.1 ± 3.3	7.1 ± 3.3	7.1 ± 3.3
	9.9 ± 3.8	9.3 ± 3.4	8.9 ± 3.3	10 ± 3.7	9 ± 2.6	8.6 ± 2.6	10.2 ± 4.4	8.9 ± 2.6	8.4 ± 2.7
30	9.7 ± 2	9.7 ± 2	9.7 ± 2	9.5 ± 1	9.5 ± 1	9.5 ± 1	9.4 ± 1.1	9.4 ± 1.1	9.4 ± 1.1
	10.6 ± 3.8	10.2 ± 3.3	10 ± 2.8	10.6 ± 3.6	10 ± 2.3	9.8 ± 2	10.7 ± 4	10 ± 2.3	9.8 ± 1.7

Table 8: $k_0 = 10$ exponentiated outliers. *Top*: Lognormal(0,1). *Middle*: $|N|(0,1)$. *Bottom*: Weibull(1,1).

C	$k=100$			$k=150$			$k=200$		
	$k^*=100$	$k^*=150$	$k^*=200$	$k^*=100$	$k^*=150$	$k^*=200$	$k^*=100$	$k^*=150$	$k^*=200$
0.001	9.7 ± 2.5	9.7 ± 2.5	9.7 ± 2.5	9.6 ± 1.1	9.6 ± 1.1	9.6 ± 1.1	9.6 ± 0.9	9.6 ± 0.9	9.6 ± 0.9
	9.7 ± 4.7	9.7 ± 3.8	9.7 ± 3	9.7 ± 4.7	9.6 ± 2.8	9.6 ± 1.9	10 ± 5.3	9.5 ± 2.5	9.6 ± 1.4
0.01	5.3 ± 4.2	5.3 ± 4.2	5.3 ± 4.2	5.5 ± 3.5	5.5 ± 3.5	5.5 ± 3.5	5.7 ± 3.3	5.7 ± 3.3	5.7 ± 3.3
	4.6 ± 6.4	5 ± 5.3	5.3 ± 4.7	4.7 ± 6.4	4.9 ± 4.8	5.4 ± 4.1	4.9 ± 6.9	5 ± 4.5	5.6 ± 3.7
1	0.3 ± 2.6	0.3 ± 2.6	0.3 ± 2.6	0.2 ± 1.6	0.2 ± 1.6	0.2 ± 1.6	0.2 ± 1.3	0.2 ± 1.3	0.2 ± 1.3
	1.7 ± 5.5	0.8 ± 4.1	0.5 ± 3.1	2.2 ± 6	0.6 ± 3.2	0.3 ± 2.5	2.8 ± 6.6	0.5 ± 3.1	0.3 ± 2.2
10	7.1 ± 4.6	7.1 ± 4.6	7.1 ± 4.6	6.4 ± 4.2	6.4 ± 4.2	6.4 ± 4.2	5.8 ± 4.4	5.8 ± 4.4	5.8 ± 4.4
	9 ± 4.6	7.7 ± 4.7	7.2 ± 4.7	9.1 ± 4.7	7.2 ± 4.5	6.6 ± 4.4	9.4 ± 5.4	6.9 ± 4.5	6 ± 4.4
50	9.9 ± 2	9.9 ± 2	9.9 ± 2	9.7 ± 0.9	9.7 ± 0.9	9.7 ± 0.9	9.7 ± 1	9.7 ± 1	9.7 ± 1
	10.4 ± 3.5	10.2 ± 3	10 ± 2.3	10.5 ± 3.4	9.9 ± 2.1	9.8 ± 1.5	10.9 ± 4.4	9.9 ± 2.1	9.7 ± 1.4
200	10 ± 1	10 ± 1	10 ± 1	10 ± 0.5	10 ± 0.5	10 ± 0.5	10 ± 0.5	10 ± 0.5	10 ± 0.5
	10.5 ± 3.1	10.2 ± 2.1	10.1 ± 1.5	10.6 ± 3.2	10.1 ± 1.5	10 ± 1.1	10.9 ± 4	10.1 ± 1.3	10 ± 1

C	$k=100$			$k=200$			$k=300$		
	$k^*=100$	$k^*=200$	$k^*=300$	$k^*=100$	$k^*=200$	$k^*=300$	$k^*=100$	$k^*=200$	$k^*=300$
0.001	9.7 ± 1	9.7 ± 1	9.7 ± 1	9.8 ± 0.6	9.8 ± 0.6	9.8 ± 0.6	9.9 ± 0.6	9.9 ± 0.6	9.9 ± 0.6
	9.5 ± 4.2	9.5 ± 3	9.5 ± 2.3	10.5 ± 5.2	9.3 ± 2.3	9.5 ± 1.6	11 ± 6	9.4 ± 2.1	9.5 ± 1.1
0.01	6.3 ± 3.2	6.3 ± 3.2	6.3 ± 3.2	7.1 ± 2.5	7.1 ± 2.5	7.1 ± 2.5	7.6 ± 2.2	7.6 ± 2.2	7.6 ± 2.2
	4.9 ± 6.8	4.5 ± 5.2	4.9 ± 4.7	6.3 ± 7.9	4.2 ± 4.5	5 ± 3.9	7.3 ± 8.5	4.4 ± 4.3	5.2 ± 3.5
1	0.3 ± 2.2	0.3 ± 2.2	0.3 ± 2.2	0.3 ± 1.7	0.3 ± 1.7	0.3 ± 1.7	0.4 ± 1.9	0.4 ± 1.9	0.4 ± 1.9
	3.2 ± 6.4	1.3 ± 4.7	0.7 ± 3.7	4.4 ± 7.5	0.9 ± 3.2	0.4 ± 2.4	4.8 ± 8.2	0.7 ± 2.8	0.3 ± 1.9
10	6.8 ± 3.9	6.8 ± 3.9	6.8 ± 3.9	4.6 ± 4.4	4.6 ± 4.4	4.6 ± 4.4	2.8 ± 4.2	2.8 ± 4.2	2.8 ± 4.2
	10 ± 3.2	9.3 ± 2.9	9 ± 2.9	10.3 ± 3.9	9 ± 2.3	8.5 ± 2.6	10.6 ± 4.7	8.7 ± 2.4	8 ± 2.8
50	9.8 ± 1.6	9.8 ± 1.6	9.8 ± 1.6	9.6 ± 1	9.6 ± 1	9.6 ± 1	9.4 ± 1.4	9.4 ± 1.4	9.4 ± 1.4
	10.7 ± 3.7	10.3 ± 2.9	10.1 ± 2.5	11.2 ± 4.4	10.1 ± 2.1	9.9 ± 1.5	11.5 ± 5.2	10 ± 1.9	9.8 ± 1.2
200	10 ± 1.2	10 ± 1.2	10 ± 1.2	9.9 ± 0.7	9.9 ± 0.7	9.9 ± 0.7	9.9 ± 0.8	9.9 ± 0.8	9.9 ± 0.8
	10.9 ± 3.7	10.3 ± 2.6	10.2 ± 2.2	11.2 ± 4.1	10.2 ± 1.8	10.1 ± 1.3	11.5 ± 4.8	10.1 ± 1.5	10 ± 1

C	$k=100$			$k=150$			$k=200$		
	$k^*=100$	$k^*=150$	$k^*=200$	$k^*=100$	$k^*=150$	$k^*=200$	$k^*=100$	$k^*=150$	$k^*=200$
0.001	9.7 ± 1.7	9.7 ± 1.7	9.7 ± 1.7	9.8 ± 1.1	9.8 ± 1.1	9.8 ± 1.1	9.8 ± 1	9.8 ± 1	9.8 ± 1
	9.4 ± 4.1	9.5 ± 3.5	9.6 ± 2.8	9.5 ± 4.2	9.4 ± 2.6	9.6 ± 2	9.8 ± 4.5	9.4 ± 2.6	9.5 ± 1.6
0.01	5.9 ± 3.5	5.9 ± 3.5	5.9 ± 3.5	6.3 ± 2.8	6.3 ± 2.8	6.3 ± 2.8	6.7 ± 2.7	6.7 ± 2.7	6.7 ± 2.7
	4.3 ± 6.3	4.4 ± 5.3	4.8 ± 4.8	4.5 ± 6.4	4.3 ± 4.7	4.8 ± 4.1	4.8 ± 6.7	4.3 ± 4.6	4.9 ± 3.9
1	0.4 ± 2.8	0.4 ± 2.8	0.4 ± 2.8	0.3 ± 1.6	0.3 ± 1.6	0.3 ± 1.6	0.3 ± 1.8	0.3 ± 1.8	0.3 ± 1.8
	2.3 ± 5.9	1.1 ± 4.7	0.7 ± 4.1	2.8 ± 6.3	0.9 ± 3.9	0.6 ± 3.4	3.3 ± 6.9	0.9 ± 3.8	0.5 ± 2.6
10	6.6 ± 4.2	6.6 ± 4.2	6.6 ± 4.2	5.6 ± 4.4	5.6 ± 4.4	5.6 ± 4.4	4.6 ± 4.5	4.6 ± 4.5	4.6 ± 4.5
	9.6 ± 3.5	8.8 ± 3.4	8.2 ± 3.6	9.7 ± 3.8	8.6 ± 3.2	7.8 ± 3.6	9.9 ± 4.3	8.4 ± 3.3	7.4 ± 3.8
50	9.8 ± 1.4	9.8 ± 1.4	9.8 ± 1.4	9.7 ± 1.2	9.7 ± 1.2	9.7 ± 1.2	9.6 ± 1.4	9.6 ± 1.4	9.6 ± 1.4
	10.5 ± 3.4	10.2 ± 2.7	10 ± 2.3	10.6 ± 3.3	10.1 ± 2.2	9.9 ± 1.8	10.8 ± 4	10 ± 2.1	9.8 ± 1.5
200	10 ± 1.2	10 ± 1.2	10 ± 1.2	10 ± 0.6	10 ± 0.6	10 ± 0.6	10 ± 0.6	10 ± 0.6	10 ± 0.6
	10.7 ± 3.6	10.4 ± 2.7	10.2 ± 2.3	10.8 ± 3.5	10.2 ± 2.1	10.1 ± 1.7	11 ± 3.9	10.2 ± 1.8	10.1 ± 1.3

Table 9: $k_0 = 10$ scaled outliers. *Top*: Lognormal(0,1). *Middle*: $|N|(0,1)$. *Bottom*: Weibull(1,1).

A.2. Proofs of the Theorems

Proof of Theorem 2.1

Considering $X_{i,n} \stackrel{d}{=} U(Y_{i,n})$, where $Y_{1,n} \leq \dots \leq Y_{n,n}$ denote the order statistics of an i.i.d. sample from the standard Pareto distribution, i.e. setting $\ell = 1$ and $\xi = 1$ in (1.2), then

$$H_{k_0,k} = \frac{k_0}{k-k_0} \log \frac{U(Y_{n-k_0,n})}{U(Y_{n-k,n})} + \frac{1}{k-k_0} \sum_{i=k_0}^{k-1} \log \frac{U(Y_{n-i,n})}{U(Y_{n-k,n})}. \quad (5.1)$$

Based on (2.2) we have

$$\frac{\log U(tx) - \log U(t)}{q_0(t)} = \frac{x^{\xi_-} - 1}{\xi_-} + Q_0(t)\Phi_{\xi_-,\rho}(x) + Q_0(t)R(t,x) \quad (5.2)$$

where $\xi_- = \min(\xi, 0)$ and the remainder $|R(t,x)| \leq \epsilon x^{\xi_- + \rho + \delta}$ for all $t \geq t_0$ and $x > 1$.

Since $Y_{n-k,n} \xrightarrow{\mathbb{P}} \infty$, we use (5.2) with $t = Y_{n-k,n}$ and $x = Y_{n-i,n}/Y_{n-k,n}$, so that with probability tending to 1

$$\begin{aligned} \frac{(k-k_0)H_{k_0,k}}{kq_0(Y_{n-k,n})} &= \underbrace{\frac{k_0}{k} \Psi_{\xi_-} \left(\frac{Y_{n-k_0,n}}{Y_{n-k,n}} \right) + \frac{1}{k} \sum_{i=k_0}^{k-1} \Psi_{\xi_-} \left(\frac{Y_{n-i,n}}{Y_{n-k,n}} \right)}_{A_{k_0,k}(n)} \\ &\quad + \underbrace{Q_0(Y_{n-k,n}) \left(\frac{k_0}{k} \Phi_{\xi_-,\rho} \left(\frac{Y_{n-k_0,n}}{Y_{n-k,n}} \right) + \frac{1}{k} \sum_{i=k_0}^{k-1} \Phi_{\xi_-,\rho} \left(\frac{Y_{n-i,n}}{Y_{n-k,n}} \right) \right)}_{B_{k_0,k}(n)} \\ &\quad + \underbrace{Q_0(Y_{n-k,n}) \left(\frac{k_0}{k} R \left(Y_{n-k,n}, \frac{Y_{n-k_0,n}}{Y_{n-k,n}} \right) + \frac{1}{k} \sum_{i=k_0}^{k-1} R \left(Y_{n-k,n}, \frac{Y_{n-i,n}}{Y_{n-k,n}} \right) \right)}_{C_{k_0,k}(n)}. \quad (5.3) \end{aligned}$$

Since $Y_{n-k,n}/(n/k) \xrightarrow{\mathbb{P}} 1$ and Q_0 is regularly varying with index ρ , $Q_0(Y_{n-k,n})/Q_0(n/k) \xrightarrow{\mathbb{P}} 1$. By (2.3) and Corollary 2.3.5, Theorem 2.3.6 and assumption (3.5.14) in *de Haan and Ferreira* (2006)

$$\lim_{k \rightarrow \infty} \sqrt{k} Q_0 \left(\frac{n}{k} \right) = \lim_{k \rightarrow \infty} \sqrt{k} Q \left(\frac{n}{k} \right) \left(\frac{1}{\rho} \mathbb{1}_{\{\rho < 0\}} + \mathbb{1}_{\{\rho = 0\}} \right) = \lambda \left(\frac{1}{\rho} \mathbb{1}_{\{\rho < 0\}} + \mathbb{1}_{\{\rho = 0\}} \right).$$

Therefore,

$$\sqrt{k} Q_0(Y_{n-k,n}) = \lambda \left(\frac{1}{\rho} \mathbb{1}_{\{\rho < 0\}} + \mathbb{1}_{\{\rho = 0\}} \right) + o_{\mathbb{P}}(1). \quad (5.4)$$

We next consider the asymptotic behaviour of $A_{k_0,k}(n)$, $B_{k_0,k}(n)$ and $C_{k_0,k}(n)$. \square

Proposition 5.1.

$$A_{k_0,k}(n) \stackrel{d}{=} \begin{cases} \frac{1}{k} \sum_{i=k_0+1}^k Z_i, & \xi \geq 0 \\ \frac{k_0}{k} (\exp(\xi \sum_{j=k_0+1}^k Z_j/j) - 1)/\xi + \frac{1}{k} \sum_{i=k_0}^{k-1} (\exp(\xi \sum_{j=i+1}^k Z_j/j) - 1)/\xi, & \xi < 0 \end{cases}$$

Proof.

$$A_{k_0,k}(n) = \frac{k_0}{k} \Psi_{\xi_-} \left(\frac{Y_{n-k_0,n}}{Y_{n-k,n}} \right) + \frac{1}{k} \sum_{i=k_0}^{k-1} \Psi_{\xi_-} \left(\frac{Y_{n-i,n}}{Y_{n-k,n}} \right).$$

When $\xi \geq 0$ we have $\Psi_{\xi_-}(x) = \log x$, and

$$\begin{aligned} A_{k_0,k}(n) &= \frac{k_0}{k} \log \frac{Y_{n-k_0,n}}{Y_{n-k,n}} + \frac{1}{k} \sum_{i=k_0}^{k-1} \log \frac{Y_{n-i,n}}{Y_{n-k,n}} \\ &\stackrel{d}{=} \frac{k_0}{k} (E_{n-k_0,n} - E_{n-k,n}) + \frac{1}{k} \sum_{i=k_0}^{k-1} (E_{n-i,n} - E_{n-k,n}) \end{aligned} \quad (5.5)$$

where $E_{1,n} \leq \dots \leq E_{n,n}$ denote the order statistics of an i.i.d. sample of size n from the standard exponential distribution.

Using the Rényi representation of exponential order statistics (see section 4.4 in (*Beirlant et al.*, 2004)) $E_{n-i,n} = \sum_{j=i+1}^n Z_j/j$ where Z_1, Z_2, \dots are i.i.d. standard exponential rv's, now yields

$$\begin{aligned} A_{k_0,k}(n) &= \frac{k_0}{k} \left(\sum_{j=k_0+1}^n \frac{Z_j}{j} - \sum_{j=k+1}^n \frac{Z_j}{j} \right) + \frac{1}{k} \sum_{i=k_0}^{k-1} \left(\sum_{j=i+1}^n \frac{Z_j}{j} - \sum_{j=k+1}^n \frac{Z_j}{j} \right) \\ &= \frac{k_0}{k} \sum_{j=k_0+1}^k \frac{Z_j}{j} + \frac{1}{k} \sum_{i=k_0}^{k-1} \sum_{j=i+1}^k \frac{Z_j}{j}. \end{aligned}$$

Interchanging the order of summation in i and j in the second summand, we obtain

$$A_{k_0,k}(n) = \frac{k_0}{k} \sum_{j=k_0+1}^k \frac{Z_j}{j} + \frac{1}{k} \sum_{j=k_0+1}^k \sum_{i=k_0}^{j-1} \frac{Z_j}{j} = \frac{1}{k} \sum_{j=k_0+1}^k Z_j$$

which completes the proof for case $\xi \geq 0$.

When $\xi < 0$ we have $\Psi_{\xi_-}(x) = \Psi_{\xi}(x)$ leading to

$$A_{k_0,k}(n) = \frac{k_0}{k\xi} \left(\left(\frac{Y_{n-k_0,n}}{Y_{n-k,n}} \right)^{\xi} - 1 \right) + \frac{1}{k\xi} \sum_{i=k_0}^{k-1} \left(\left(\frac{Y_{n-i,n}}{Y_{n-k,n}} \right)^{\xi} - 1 \right)$$

$$\begin{aligned}
&= \frac{k_0}{k\xi} \left(\exp \left(\xi \log \frac{Y_{n-k_0,n}}{Y_{n-k,n}} \right) - 1 \right) + \frac{1}{k\xi} \sum_{i=k_0}^{k-1} \left(\exp \left(\xi \log \frac{Y_{n-i,n}}{Y_{n-k,n}} \right) - 1 \right) \\
&\stackrel{d}{=} \frac{k_0}{k\xi} \left(\exp(\xi[E_{n-k_0,n} - E_{n-k,n}]) - 1 \right) + \frac{1}{k\xi} \sum_{i=k_0}^{k-1} \left(\exp(\xi[E_{n-i,n} - E_{n-k,n}]) - 1 \right). \tag{5.6}
\end{aligned}$$

Again using the Rényi representation gives

$$A_{k_0,k}(n) = \frac{k_0}{k} \left(\exp(\xi \sum_{j=k_0+1}^k Z_j/j) - 1 \right) / \xi + \frac{1}{k} \sum_{i=k_0}^{k-1} \left(\exp(\xi \sum_{j=i+1}^k Z_j/j) - 1 \right) / \xi,$$

which completes the proof for case $\xi < 0$. \square

Proposition 5.2. *As $k, n \rightarrow \infty$, $k/n \rightarrow 0$ and $k_0 = o(k)$*

$$B_{k_0,k}(n) = c_{\xi_-, \rho} + o_{\mathbb{P}}(1)$$

$$c_{\xi_-, \rho} = \begin{cases} \frac{1}{1-\xi_--\rho} \left(1 - \left(\frac{k_0}{k}\right)^{1-\xi_--\rho}\right), & \rho < 0 \\ \frac{1}{\xi_-(1-\xi_-)^2} \left(1 - \left(\frac{k_0}{k}\right)^{1-\xi_-}\right) - \frac{1}{1-\xi_-} \left(\frac{k_0}{k}\right)^{1-\xi_-} \log \frac{k_0}{k}, & \rho = 0, \xi_- < 0 \\ \left(1 - \frac{k_0}{k}\right) - \frac{k_0}{k} \log \frac{k_0}{k}, & \rho = 0, \xi_- = 0. \end{cases} \tag{5.7}$$

Hence, with (5.4),

$$Q_0(Y_{n-k,n})B_{k_0,k}(n) = \lambda \left(\frac{1}{\rho} \mathbb{1}_{\{\rho < 0\}} + \mathbb{1}_{\{\rho = 0\}} \right) \frac{c_{\xi_-, \rho}}{\sqrt{k}} + o_{\mathbb{P}}(k^{-1/2})$$

Proof.

$$B_{k_0,k}(n) = \frac{k_0}{k} \Phi_{\xi_-, \rho} \left(\frac{Y_{n-k_0,n}}{Y_{n-k,n}} \right) + \frac{1}{k} \sum_{i=k_0}^{k-1} \Phi_{\xi_-, \rho} \left(\frac{Y_{n-i,n}}{Y_{n-k,n}} \right).$$

In case $\rho < 0$, then

$$B_{k_0,k}(n) = \frac{1}{\xi_- + \rho} \left(\frac{k_0}{k} \left(\frac{Y_{n-k_0,n}}{Y_{n-k,n}} \right)^{\xi_- + \rho} + \frac{1}{k} \sum_{i=k_0}^{k-1} \left(\frac{Y_{n-i,n}}{Y_{n-k,n}} \right)^{\xi_- + \rho} - 1 \right).$$

By Lemma 5.4 below, $B_{k_0,k} = 1/(1 - \xi_- - \rho)(1 - (k_0/k)^{1-\xi_- - \rho}) + o_{\mathbb{P}}(1)$.

In case $\xi_- < 0$, $\rho = 0$,

$$B_{k_0,k}(n) = \frac{k_0}{k\xi_-} \left(\frac{Y_{n-k_0,n}}{Y_{n-k,n}} \right)^{\xi_-} \log \frac{Y_{n-k_0,n}}{Y_{n-k,n}} + \frac{1}{k\xi_-} \sum_{i=k_0}^{k-1} \left(\frac{Y_{n-i,n}}{Y_{n-k,n}} \right)^{\xi_-} \log \frac{Y_{n-i,n}}{Y_{n-k,n}}$$

By Lemma 5.5 below, $B_{k_0,k} = 1/(\xi_-(1-\xi_-)^2)(1-(k_0/k)^{\xi_-}) - 1/(1-\xi_-)((k_0/k)^{\xi_-} \log(k_0/k)) + o_{\mathbb{P}}(1)$.

In case $\xi_- = 0, \rho = 0$,

$$B_{k_0,k}(n) = \frac{k_0}{2k} \left(\log \frac{Y_{n-k_0,n}}{Y_{n-k,n}} \right)^2 + \frac{1}{2k} \sum_{i=k_0}^{k-1} \left(\log \frac{Y_{n-i,n}}{Y_{n-k,n}} \right)^2.$$

By Lemma 5.6 below, $B_{k_0,k} = 1 - (k_0/k) - (k_0/k) \log(k_0/k) + o_{\mathbb{P}}(1)$. □

The following Proposition concerning $C_{k_0,k}(n)$ in (5.3) ends the proof of Theorem 2.1.

Proposition 5.3. *As $k, n \rightarrow \infty$, $k/n \rightarrow 0$ and $k_0 = o(k)$*

$$C_{k_0,k}(n) = o_{\mathbb{P}}(1).$$

Thus, in view of (5.4),

$$Q_0(Y_{n-k,n})C_{k_0,k}(n) = o_{\mathbb{P}}(k^{-1/2}).$$

Proof.

$$C_{k_0,k}(n) = \frac{k_0}{k} R\left(Y_{n-k,n}, \frac{Y_{n-k_0,n}}{Y_{n-k,n}}\right) + \frac{1}{k} \sum_{i=k_0}^{k-1} R\left(Y_{n-k,n}, \frac{Y_{n-i,n}}{Y_{n-k,n}}\right).$$

Since $Y_{n-k,n} \xrightarrow{\mathbb{P}} 1$, with probability tending to 1 we have

$$\left| R\left(Y_{n-k,n}, \frac{Y_{n-i,n}}{Y_{n-k,n}}\right) \right| \leq \epsilon \left(\frac{Y_{n-i,n}}{Y_{n-k,n}} \right)^{\xi_- + \rho + \delta}, \quad i = k_0, \dots, k-1.$$

Therefore,

$$|C_{k_0,k}(n)| \leq \epsilon \underbrace{\left| \frac{k_0}{k} \left(\frac{Y_{n-k_0,n}}{Y_{n-k,n}} \right)^{\xi_- + \rho + \delta} + \frac{1}{k} \sum_{i=k_0}^{k-1} \left(\frac{Y_{n-i,n}}{Y_{n-k,n}} \right)^{\xi_- + \rho + \delta} \right|}_{C_{k_0,k}^*(n)}. \quad (5.8)$$

If $\xi_- + \rho < 0$, then for δ sufficiently small, $\xi_- + \rho + \delta < 0$.

By Lemma 5.4 below,

$$C_{k_0,k}^* = 1 + \frac{1}{(1-\xi_- - \rho - \delta)} \left(1 - \left(\frac{k_0}{k} \right)^{1-\xi_- - \rho - \delta} \right) + o_{\mathbb{P}}(1)$$

If $\xi_- + \rho = 0$, then for every $1 > \delta > 0$,

$$|C_{k_0,k}^*| \leq \frac{1}{k} \sum_{i=0}^{k-1} \left(\frac{Y_{n-i,n}}{Y_{n-k,n}} \right)^{\delta} \stackrel{d}{=} \frac{1}{k} \sum_{i=0}^{k-1} U_{i,k}^{-\delta} = \frac{1}{1-\delta} + o_{\mathbb{P}}(1)$$

where $U_{1,k} \leq \dots \leq U_{k,k}$ denote the order statistics of uniform (0,1) i.i.d. sample of length k and the convergence follows from the law of large numbers.

Thus, $C_{k_0,k}^* = O_{\mathbb{P}}(1)$ which in view of (5.8) implies $C_{k_0,k} = o_{\mathbb{P}}(1)$. \square

Proof of Theorem 2.2 Note that

$$1 - T_{k_0,k} = \frac{(k_0 + 1) \log \frac{X_{n-k_0,n}}{X_{n-k_0-1,n}}}{(k - k_0)H_{k_0,k}} = \frac{V_{k_0+1}}{(k - k_0)H_{k_0,k}}, \quad (5.9)$$

with V_{k_0+1} defined in (1.5).

With the same notations as in the proof of Theorem 2.1, we have

$$\begin{aligned} V_{k_0+1} &= (k_0 + 1) \log \frac{U(Y_{n-k_0,n})}{U(Y_{n-k_0-1,n})} \\ &= (k_0 + 1) \log \frac{U\left(\frac{Y_{n-k_0,n}}{Y_{n-k_0-1,n}}\right)}{U\left(Y_{n-k_0-1,n}\right)}. \end{aligned} \quad (5.10)$$

Using (5.2) with $t = Y_{n-k_0-1,n}$ and $x = \frac{Y_{n-k_0,n}}{Y_{n-k_0-1,n}}$ we obtain

$$\begin{aligned} V_{k_0+1} &= (k_0 + 1)q_0(Y_{n-k_0-1,n}) \left\{ \Psi_{\xi_-} \left(\frac{Y_{n-k_0,n}}{Y_{n-k_0-1,n}} \right) + Q_0(Y_{n-k_0-1,n}) \Phi_{\xi_-,\rho} \left(\frac{Y_{n-k_0,n}}{Y_{n-k_0-1,n}} \right) \right. \\ &\quad \left. + Q_0(Y_{n-k_0-1,n}) R \left(Y_{n-k_0-1,n}, \frac{Y_{n-k_0,n}}{Y_{n-k_0-1,n}} \right) \right\}, \end{aligned} \quad (5.11)$$

where $|R \left(Y_{n-k_0-1,n}, \frac{Y_{n-k_0,n}}{Y_{n-k_0-1,n}} \right)| \leq \epsilon \left(\frac{Y_{n-k_0,n}}{Y_{n-k_0-1,n}} \right)^{\xi_- + \rho + \delta}$.

Since $Y_{n-k_0,n}/(n/k_0) = O_{\mathbb{P}}(1)$ when $k_0 = o(k)$, we have

$$\Phi_{\xi_-,\rho} \left(\frac{Y_{n-k_0,n}}{Y_{n-k_0-1,n}} \right) = O_{\mathbb{P}}(1) \quad R \left(Y_{n-k_0-1,n}, \frac{Y_{n-k_0,n}}{Y_{n-k_0-1,n}} \right) = o_{\mathbb{P}}(1).$$

A representation of the denominator of the right hand side of (5.9) follows from Theorem 2.1. We now combine (5.10) with that result.

Since Q_0 is regularly varying with index $\rho \leq 0$, i.e. $Q_0(x) = x^\rho \ell_0(x)$ for some slowly varying function ℓ_0 , we invoke Potter bounds so that for any $\delta_1, \delta_2 > 0$ and t large enough

$$\frac{\ell_0(tx)}{\ell_0(t)} \leq (1 + \delta_1)x^{\delta_2}, \quad \text{with } x > 1,$$

(see for instance Proposition B.1.9 in de Haan and Ferreira (2006)) so that for any $\delta > 0$

$$\begin{aligned}
(k_0 + 1) \frac{Q_0(Y_{n-k_0-1,n})}{Q_0(Y_{n-k,n})} &= (k_0 + 1) \frac{Q_0\left(\frac{Y_{n-k_0-1,n}}{Y_{n-k,n}} Y_{n-k,n}\right)}{Q_0(Y_{n-k,n})} \\
&= (k_0 + 1) \left(\frac{Y_{n-k_0-1,n}}{Y_{n-k,n}}\right)^\rho \frac{\ell_0\left(\frac{Y_{n-k_0-1,n}}{Y_{n-k,n}} Y_{n-k,n}\right)}{\ell_0(Y_{n-k,n})} \\
&= O_{\mathbb{P}}\left(k_0 \left(\frac{k}{k_0}\right)^{\rho+\delta}\right).
\end{aligned}$$

Since $Y_{n-k,n}/(n/k) \rightarrow_{\mathbb{P}} 1$, $Q_0(Y_{n-k,n}) = O_{\mathbb{P}}(1/\sqrt{k})$ using the assumption $\sqrt{k}Q_0(n/k) \rightarrow \lambda$, from which

$$(k_0 + 1)Q_0(Y_{n-k_0-1,n}) = Q_0(Y_{n-k,n})O_{\mathbb{P}}\left(k_0 \left(\frac{k}{k_0}\right)^{\rho+\delta}\right) = O_{\mathbb{P}}\left(k^{-1/2} k_0 \left(\frac{k}{k_0}\right)^{\rho+\delta}\right). \quad (5.12)$$

Furthermore, using (2.3.18) in de Haan and Ferreira (2006) stating that

$$\frac{q_0(tx)}{q_0(t)} = x^{\xi_-} \left(1 + Q_0(t)x^{\xi_-}\Psi_\rho(x) + Q_0(t)\tilde{R}(t,x)\right),$$

with $|\tilde{R}(t,x)| \leq \epsilon x^{\xi_- + \rho + \delta}$, we obtain with $t = Y_{n-k,n}$ and $x = \frac{Y_{n-k_0-1,n}}{Y_{n-k,n}}$ that

$$\left(\frac{Y_{n-k,n}}{Y_{n-k_0-1,n}}\right)^{\xi_-} \frac{q_0(Y_{n-k_0-1,n})}{q_0(Y_{n-k,n})} = 1 + Q_0(Y_{n-k,n})\Psi_\rho\left(\frac{Y_{n-k_0-1,n}}{Y_{n-k,n}}\right) + Q_0(Y_{n-k,n})\tilde{R}\left(Y_{n-k,n}, \frac{Y_{n-k_0-1,n}}{Y_{n-k,n}}\right). \quad (5.13)$$

Also

$$\Psi_\rho\left(\frac{Y_{n-k_0-1,n}}{Y_{n-k,n}}\right) = \begin{cases} O_{\mathbb{P}}(1) & \text{if } \rho < 0, \\ O_{\mathbb{P}}(\log(k/k_0)) & \text{if } \rho = 0. \end{cases} \quad (5.14)$$

Also,

$$|\tilde{R}\left(Y_{n-k,n}, \frac{Y_{n-k_0-1,n}}{Y_{n-k,n}}\right)| \leq \epsilon \left(\frac{Y_{n-k_0-1,n}}{Y_{n-k,n}}\right)^{\rho+\delta} = o_{\mathbb{P}}\left((k/k_0)^{\rho+\delta}\right). \quad (5.15)$$

Hence, combining (5.13), (5.14) and (5.15) we obtain

$$\left(\frac{k_0 + 1}{k}\right)^{\xi_-} \frac{q_0(Y_{n-k_0-1,n})}{q_0(Y_{n-k,n})} = 1 + o_{\mathbb{P}}\left(k^{-1/2}(k/k_0)^{\rho+\delta}\right). \quad (5.16)$$

Next, with the method of proof developed in Proposition 5.1,

$$(k_0 + 1)\Psi_{\xi_-}\left(\frac{Y_{n-k_0-1,n}}{Y_{n-k_0-1,n}}\right) = \begin{cases} Z_{k_0}, & \text{if } \xi_- = 0, \\ \frac{k_0+1}{\xi_-} \left(e^{\xi_- \frac{Z_{k_0}}{k_0+1}} - 1\right), & \text{if } \xi_- < 0. \end{cases} \quad (5.17)$$

By Theorem 2.1, $(k - k_0)H_{k_0,k}/q_0(Y_{n-k,n}) \stackrel{d}{=} kZ_{k_0,k} + O_{\mathbb{P}}(k^{-1/2})$ where

$$Z_{k_0,k} = \begin{cases} \sum_{j=k_0+1}^k Z_j, & \xi_- = 0 \\ k_0(\exp(\xi_- \sum_{j=k_0+1}^k Z_j/j) - 1)/\xi_- + \sum_{i=k_0}^{k-1} (\exp(\xi_- \sum_{j=i+1}^k Z_j/j) - 1)/\xi_- & \xi_- < 0. \end{cases} \quad (5.18)$$

The result now follows combining (5.9), (5.11), (5.12), (5.16), (5.17) and (5.18). \square

Lemma 5.4. *With Y_1, \dots, Y_n an i.i.d. sample from the standard Pareto distribution, we have for any $\beta < 0$, as $k, n \rightarrow \infty$, $k/n \rightarrow 0$ and $k_0 = o(k)$*

$$\left| \frac{k_0}{k} \left(\frac{Y_{n-k_0,n}}{Y_{n-k,n}} \right)^\beta + \frac{1}{k} \sum_{i=k_0}^{k-1} \left(\frac{Y_{n-i,n}}{Y_{n-k,n}} \right)^\beta - 1 - \frac{\beta}{1-\beta} \left(1 - \left(\frac{k_0}{k} \right)^{1-\beta} \right) \right| \xrightarrow{\mathbb{P}} 0. \quad (5.19)$$

Proof.

$$\begin{aligned} \frac{k_0}{k} \left(\frac{Y_{n-k_0,n}}{Y_{n-k,n}} \right)^\beta + \frac{1}{k} \sum_{i=k_0}^{k-1} \left(\frac{Y_{n-i,n}}{Y_{n-k,n}} \right)^\beta &= \frac{1}{k} \sum_{i=0}^{k-1} \left(\frac{Y_{n-i,n}}{Y_{n-k,n}} \right)^\beta - \frac{1}{k} \sum_{i=0}^{k_0-1} \left(\left(\frac{Y_{n-i,n}}{Y_{n-k,n}} \right)^\beta - \left(\frac{Y_{n-k_0,n}}{Y_{n-k,n}} \right)^\beta \right) \\ &\stackrel{d}{=} \underbrace{\frac{1}{k} \sum_{i=1}^k \left(\frac{\Gamma_i}{\Gamma_{k+1}} \right)^{-\beta}}_{\Delta_k} - \underbrace{\frac{1}{k} \sum_{i=1}^{k_0} \left(\left(\frac{\Gamma_i}{\Gamma_{k+1}} \right)^{-\beta} - \left(\frac{\Gamma_{k_0+1}}{\Gamma_{k+1}} \right)^{-\beta} \right)}_{\Delta_{k_0,k}}, \end{aligned}$$

where $\Gamma_j = \sum_{i=1}^j E_i$ ($j = 1, 2, \dots$).

By Lemma C.4 in *Bhattacharya et al. (2019)*, $\Delta_k \xrightarrow{\mathbb{P}} 1/(1-\beta)$.

If $k_0 = k_0(n) \leq M$ for all n , then $\Delta_{k_0,k} = o_{\mathbb{P}}(1)$ and hence the proof of (5.19) follows.

If $k_0 = k_0(n) \rightarrow \infty$, then

$$\Delta_{k_0,k} - \frac{\beta}{1-\beta} \left(\frac{k_0}{k} \right)^{1-\beta} = o_{\mathbb{P}}(1) \quad (5.20)$$

since

$$\begin{aligned} \left| \Delta_{k_0,k} - \frac{\beta}{1-\beta} \left(\frac{k_0}{k} \right)^{1-\beta} \right| &= \left| \frac{1}{k} \sum_{i=1}^{k_0} \left(\left(\frac{\Gamma_i}{\Gamma_{k+1}} \right)^{-\beta} - \left(\frac{\Gamma_{k_0+1}}{\Gamma_{k+1}} \right)^{-\beta} \right) - \frac{\beta}{1-\beta} \left(\frac{k_0}{k} \right)^{1-\beta} \right| \\ &= \left(\frac{k_0}{k} \right)^{1-\beta} \left| \left(\frac{\Gamma_{k_0+1}/k_0}{\Gamma_{k+1}/k} \right)^{-\beta} \left(\underbrace{\frac{1}{k_0} \sum_{i=1}^{k_0} \left(\frac{\Gamma_i}{\Gamma_{k_0+1}} \right)^{-\beta}}_{\Delta_{k_0}} - 1 \right) - \frac{\beta}{1-\beta} \right|. \end{aligned} \quad (5.21)$$

where $((k\Gamma_{k_0+1})/(k_0\Gamma_{k+1}))^{-\beta} \xrightarrow{\mathbb{P}} 1$ and $\Delta_{k_0} \xrightarrow{\mathbb{P}} \beta/(1-\beta)$ and follows from Lemmas C.3 and C.4 in *Bhattacharya et al. (2019)* respectively. This completes the proof. \square

Lemma 5.5. *With $\beta < 0$ and*

$$B_{k_0,k}(n) = \frac{k_0}{k} \left(\frac{Y_{n-k_0,n}}{Y_{n-k,n}} \right)^\beta \log \frac{Y_{n-k_0,n}}{Y_{n-k,n}} + \frac{1}{k} \sum_{i=k_0}^{k-1} \left(\frac{Y_{n-i,n}}{Y_{n-k,n}} \right)^\beta \log \frac{Y_{n-i,n}}{Y_{n-k,n}},$$

we have as $k, n \rightarrow \infty$, $k/n \rightarrow 0$ and $k_0 = o(k)$

$$\left| B_{k_0,k}(n) - \frac{1}{(1-\beta)^2} + \frac{\beta}{1-\beta} \left(\frac{k_0}{k} \right)^{1-\beta} \left(\frac{1}{\beta(1-\beta)} + \log \frac{k}{k_0} \right) \right| \xrightarrow{\mathbb{P}} 0. \quad (5.22)$$

Proof. Here

$$\begin{aligned} B_{k_0,k}(n) &\stackrel{d}{=} \frac{k_0}{k} \left(\frac{\Gamma_{k_0+1}}{\Gamma_{k+1}} \right)^{-\beta} \log \frac{\Gamma_{k+1}}{\Gamma_i} + \frac{1}{k} \sum_{i=k_0+1}^k \left(\frac{\Gamma_i}{\Gamma_{k+1}} \right)^{-\beta} \log \frac{\Gamma_{k+1}}{\Gamma_i} \\ &= \underbrace{\frac{1}{k} \sum_{i=1}^k \left(\frac{\Gamma_i}{\Gamma_{k+1}} \right)^{-\beta} \log \frac{\Gamma_{k+1}}{\Gamma_i}}_{\Delta_k} - \underbrace{\frac{1}{k} \sum_{i=1}^{k_0} \left(\left(\frac{\Gamma_i}{\Gamma_{k+1}} \right)^{-\beta} \log \frac{\Gamma_{k+1}}{\Gamma_i} - \left(\frac{\Gamma_{k_0+1}}{\Gamma_{k+1}} \right)^{-\beta} \log \frac{\Gamma_{k+1}}{\Gamma_{k_0+1}} \right)}_{\Delta_{k_0,k}}. \end{aligned}$$

By Lemma C.4 in *Bhattacharya et al. (2019)*, $\Delta_k \xrightarrow{\mathbb{P}} 1/(1-\beta)^2$ as $k \rightarrow \infty$.

We next show that

$$\left| \Delta_{k_0,k} - \frac{1}{(1-\beta)^2} \left(\frac{k_0}{k} \right)^{1-\beta} - \frac{\beta}{1-\beta} \left(\frac{k_0}{k} \right)^{1-\beta} \log \frac{k}{k_0} \right| \xrightarrow{\mathbb{P}} 0, \quad (5.23)$$

which will complete the proof of the Lemma.

If $k_0 = k_0(n) \leq M$ for all n , then using $\Gamma_i/\Gamma_k = O_{\mathbb{P}}(1/k)$, one can show $\Delta_{k_0,k} = o_{\mathbb{P}}(1)$.

In case $k_0 = k_0(n) \rightarrow \infty$, we write

$$\begin{aligned} \Delta_{k_0,k} &= \left(\frac{\Gamma_{k_0+1}}{\Gamma_{k+1}} \right)^{-\beta} \frac{1}{k} \sum_{i=1}^{k_0} \left(\left(\frac{\Gamma_i}{\Gamma_{k_0+1}} \right)^{-\beta} \log \frac{\Gamma_{k+1}}{\Gamma_i} - \log \frac{\Gamma_{k+1}}{\Gamma_{k_0+1}} \right) \\ &= \underbrace{\left(\frac{\Gamma_{k_0+1}}{\Gamma_{k+1}} \right)^{-\beta} \frac{1}{k} \sum_{i=1}^{k_0} \left(\frac{\Gamma_i}{\Gamma_{k_0+1}} \right)^{-\beta} \log \frac{\Gamma_{k_0+1}}{\Gamma_i}}_{\Delta_{1,k_0,k}} + \underbrace{\left(\frac{\Gamma_{k_0+1}}{\Gamma_{k+1}} \right)^{-\beta} \log \frac{\Gamma_{k+1}}{\Gamma_{k_0+1}} \frac{1}{k} \sum_{i=1}^{k_0} \left(\left(\frac{\Gamma_i}{\Gamma_{k_0+1}} \right)^{-\beta} - 1 \right)}_{\Delta_{2,k_0,k}}, \end{aligned}$$

where

$$\left| \Delta_{1,k_0,k} - \frac{1}{(1-\beta)^2} \left(\frac{k_0}{k} \right)^{1-\beta} \right| = \left(\frac{k_0}{k} \right)^{1-\beta} \left| \left(\frac{\Gamma_{k_0+1}/k_0}{\Gamma_{k+1}/k} \right)^{-\beta} \frac{1}{k_0} \sum_{i=1}^{k_0} \left(\frac{\Gamma_{k_0+1}}{\Gamma_i} \right)^{-\beta} \log \frac{\Gamma_i}{\Gamma_{k_0+1}} - \frac{1}{(1-\beta)^2} \right|.$$

By Lemma C.3 in *Bhattacharya et al. (2019)*, $((k\Gamma_{k_0+1})/(k_0\Gamma_{k+1}))^{-\beta} \xrightarrow{\mathbb{P}} 1$. Using ideas similar to proof of Lemma C.4 in *Bhattacharya et al. (2019)*, $(1/k_0) \sum_{i=1}^{k_0} (\Gamma_{k_0+1}/\Gamma_i)^{-\beta} \log(\Gamma_i/\Gamma_{k_0+1}) \xrightarrow{\mathbb{P}} 1/(1-\beta)^2$. Therefore,

$$\Delta_{1,k_0,k} - \frac{1}{(1-\beta)^2} \left(\frac{k_0}{k}\right)^{1-\beta} = o_{\mathbb{P}}(1). \quad (5.24)$$

Furthermore,

$$\left| \Delta_{2,k_0,k} - \frac{\beta}{1-\beta} \left(\frac{k_0}{k}\right)^{1-\beta} \log \frac{k}{k_0} \right| = \delta_{k_0,k} \left| \left(\frac{\Gamma_{k_0+1}/k_0}{\Gamma_{k+1}/k}\right)^{-\beta} \frac{\log(\Gamma_{k+1}/\Gamma_{k_0+1})}{\log(k/k_0)} \frac{1}{k_0} \underbrace{\sum_{i=1}^{k_0} \left(\left(\frac{\Gamma_i}{\Gamma_{k_0+1}}\right)^{-\beta} - 1 \right)}_{\Delta_{2,k_0}} - \frac{\beta}{1-\beta} \right|$$

where $\delta_{k_0,k} = (k_0/k)^{1-\beta} \log(k/k_0) \leq 1$.

If $k_0 = k_0(n) \leq M$ for all n , then $\Delta_{2,k_0,k} = o_{\mathbb{P}}(1)$ since then $\Gamma_{k_0+1}/\Gamma_{k+1} = O(1/k)$.

In case $k_0 = k_0(n) \rightarrow \infty$, by Lemma C.4 in *Bhattacharya et al. (2019)*, $\Delta_{2,k_0} = \beta/(1-\beta) + o_{\mathbb{P}}(1)$.

Using ideas similar to proof of Lemma C.3 in *Bhattacharya et al. (2019)*,

$$\left(\frac{\Gamma_{k_0+1}/k_0}{\Gamma_{k+1}/k}\right)^{-\beta} \log \frac{\Gamma_{k+1}}{\Gamma_{k_0+1}} \left(\log \frac{k}{k_0}\right)^{-1} \xrightarrow{\mathbb{P}} 1.$$

Therefore,

$$\Delta_{2,k_0,k} - \frac{\beta}{(1-\beta)} \left(\frac{k_0}{k}\right)^{1-\beta} \log \frac{k}{k_0} = o_{\mathbb{P}}(1). \quad (5.25)$$

In view of (5.24) and (5.25), the proof of (5.23) follows. \square

Lemma 5.6. For $\beta < 0$ and

$$B_{k_0,k}(n) = \frac{k_0}{2k} \left(\log \frac{Y_{(n-k_0,n)}}{Y_{n-k,n}} \right)^2 + \frac{1}{2k} \sum_{i=k_0}^{k-1} \left(\log \frac{Y_{(n-i,n)}}{Y_{n-k,n}} \right)^2,$$

we have as $k, n \rightarrow \infty$, $k/n \rightarrow 0$ and $k_0 = o(k)$

$$\left| B_{k_0,k}(n) - 1 + \frac{k_0}{k} \left(1 + \log \frac{k}{k_0} \right) \right| \xrightarrow{\mathbb{P}} 0. \quad (5.26)$$

Proof. Here

$$\begin{aligned} B_{k_0,k}(n) &\stackrel{d}{=} \frac{k_0}{2k} \left(\log \frac{\Gamma_{k+1}}{\Gamma_{k_0+1}} \right)^2 + \frac{1}{2k} \sum_{i=k_0+1}^k \left(\log \frac{\Gamma_{k+1}}{\Gamma_i} \right)^2 \\ &= \underbrace{\frac{1}{2k} \sum_{i=1}^k \left(\log \frac{\Gamma_{k+1}}{\Gamma_i} \right)^2}_{\Delta_k} - \underbrace{\frac{1}{2k} \sum_{i=1}^{k_0} \left(\left(\log \frac{\Gamma_{k+1}}{\Gamma_i} \right)^2 - \left(\log \frac{\Gamma_{k+1}}{\Gamma_{k_0+1}} \right)^2 \right)}_{\Delta_{k_0,k}}. \end{aligned}$$

By using ideas similar to proof of Lemma C.4 in *Bhattacharya et al. (2019)*, $\Delta_k \xrightarrow{\mathbb{P}} 1$.
If $k_0 = k_0(n) \leq M$ for all n , then using $\Gamma_i/\Gamma_k = O_{\mathbb{P}}(1/k)$, one can show $\Delta_{k_0,k} = o_{\mathbb{P}}(1)$.
If $k_0 = k_0(n) \rightarrow \infty$,

$$\left| \Delta_{k_0,k} - \frac{k_0}{k} \left(1 + \log \frac{k}{k_0} \right) \right| \xrightarrow{\mathbb{P}} 0. \quad (5.27)$$

To this end we write

$$\begin{aligned} \Delta_{k_0,k} &= \frac{1}{2k} \sum_{i=1}^{k_0} \left(\left(\log \frac{\Gamma_{k_0+1}}{\Gamma_i} + \log \frac{\Gamma_{k+1}}{\Gamma_{k_0+1}} \right)^2 - \left(\log \frac{\Gamma_{k+1}}{\Gamma_{k_0+1}} \right)^2 \right) \\ &= \underbrace{\frac{1}{2k} \sum_{i=1}^{k_0} \left(\log \frac{\Gamma_{k_0+1}}{\Gamma_i} \right)^2}_{\Delta_{1,k_0,k}} + \underbrace{\log \frac{\Gamma_{k+1}}{\Gamma_{k_0+1}} \frac{1}{k} \sum_{i=1}^{k_0} \log \frac{\Gamma_{k_0+1}}{\Gamma_i}}_{\Delta_{2,k_0,k}}. \end{aligned}$$

Using ideas of the proof of Lemma C.4 in *Bhattacharya et al. (2019)*, we have

$$\left| \Delta_{1,k_0,k} - \frac{k_0}{k} \right| = \frac{k_0}{k} \left| \underbrace{\frac{1}{2k_0} \sum_{i=1}^{k_0} \left(\log \frac{\Gamma_{k_0+1}}{\Gamma_i} \right)^2}_{\Delta_{k_0}} - 1 \right| = o_{\mathbb{P}}(1). \quad (5.28)$$

Furthermore

$$\left| \Delta_{2,k_0,k} - \frac{k_0}{k} \log \frac{k}{k_0} \right| = \frac{k_0}{k} \log \frac{k}{k_0} \left| \frac{\log(\Gamma_{k+1}/\Gamma_{k_0+1})}{\log(k/k_0)} \frac{1}{k_0} \sum_{i=1}^{k_0} \log \frac{\Gamma_{k_0+1}}{\Gamma_i} - 1 \right| = o_{\mathbb{P}}(1) \quad (5.29)$$

where $\log(\Gamma_{k+1}/\Gamma_{k_0+1})/\log(k/k_0) \xrightarrow{\mathbb{P}} 1$ follows from Lemma C.3 in *Bhattacharya et al. (2019)*.

Using ideas similar to proof of Lemma C.4 in *Bhattacharya et al. (2019)*. $(1/k_0) \sum_{i=1}^{k_0} \log(\Gamma_{k_0+1}/\Gamma_i) = o_{\mathbb{P}}(1)$.

In view of (5.28) and (5.29), the proof of Relation (5.27) follows. \square